

FRACTURE TOUGHNESS OF QUASI-ISOTROPIC AND CROSSPLIED LAMINATES USING J-INTEGRAL APPROACH

A Thesis submitted
in Partial Fulfilment of the Requirements
for the degree of
MASTER OF TECHNOLOGY

1025

BY

K. SRINIVASAN

to the

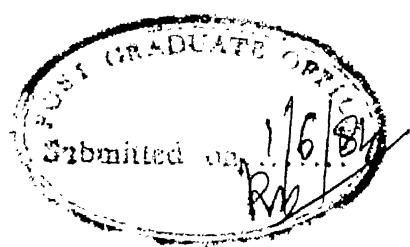
DEPARTMENT OF MECHANICAL ENGINEERING
INDIAN INSTITUTE OF TECHNOLOGY, KANPUR
MAY, 1984

10 JUL 1984

83405

ME1984-M-SRI-FRA

CERTIFICATE



This is to certify that the thesis entitled
 "FRACTURE TOUGHNESS OF QUASI-ISOTROPIC AND CROSSPLIED
 LAMINATES USING J-INTEGRAL APPROACH", by K. SRINIVASAN
 is a record of work carried out under our supervision
 and has not been submitted elsewhere for a degree.


 B.D. AGARWAL
 Professor
 Department of Mechanical Engg.
 Indian Institute of Technology
 Kanpur-208016


 Prashant Kumar

PRASHANT KUMAR
 Assistant Professor
 Department of Mech. E
 Indian Institute of
 Kanpur-208016

POST GRADUATE SECTION.	
This thesis has been approved	
for the award of the Degree of	
Master of Philosophy (M.Phil.)	
in accordance with the	
regulations of the Indian	
Institute of Technology Kanpur.	
Dated, 11-6-84	

(M.Phil.)

ACKNOWLEDGEMENT

I express my deep sense of gratitude to Professors B.D. Agarwal and Prashant Kumar for their valuable guidance throughout the present work. Their generous attitude has been a constant source of inspiration and encouragement.

I am indebted to Dr. B.S. Patro for having taught me the testing procedure and data analysis. Special thanks are to my friends Messers R.K. Nakrani, R.K. Gupta, B.K. Mishra, S.K. Khanna, K.S. Babu who had helped me during various stages.

Thanks are due to Messers S.L. Srivastava, D.K. Sarkar, Swaran Singh, S.N. Dwivedy, R.S. Shukla, B.D. Pandey, S.N. Yadav for their cooperation and help rendered throughout the experimental investigations. I highly commend Mr. B.K. Jain of Advanced Centre for Materials Science who helped me a lot in carrying out the testing.

This work was partially supported by the Aeronautics Research and Development Board (Structures Panel). I owe a sense of gratitude to the Head, Mechanical Engineering Department for having provided me the teaching assistantship right from the second semester till now which had been of great use to me.

I am indebted to my friends Messers G. Kumaravel, V. Palaniappan, V. Mohan, S.C.R. Chandar, K. Raghavan, Padma Raghavan, V. Muruganandam, V. Kandasamy, A. Subramanian all of whom provided me a homely atmosphere and having made my stay here an enjoyable one.

I shall fall back from my duty if I do not recall the hardships of my parents to raise me to these heights. A record of appreciation is due to my brother K. Raghavan and sisters K. Sudha, K. Ladha and K. Rama for their constant encouragement.

Last but not the least thanks are due to Mr. D.P. Saini for the excellent typing of the manuscript.

K. SRINIVASAN.

TABLE OF CONTENTS

	<u>Page</u>
LIST OF FIGURES	(vi)
NOMENCLATURE	(x)
ABSTRACT	(xii)
CHAPTER I : INTRODUCTION	1
1.1 : COMPOSITES	1
1.2 : FRACTURE MECHANICS OF COMPOSITES	2
1.3 : BASIS FOR J-INTEGRAL	5
1.4 : J-INTEGRAL ESTIMATION PROCEDURES	14
1.5 : SCOPE OF THE PRESENT WORK	18
CHAPTER II : EXPERIMENTAL DETAILS	19
2.1 : TESTING SYSTEM	24
CHAPTER III : RESULTS AND DISCUSSION	29
3.1 : QUASI-ISOTROPIC LAMINATES	29
3.2 : CROSS-PLY LAMINATES	46
3.3 : FACTORS AFFECTING THE FRACTURE TOUGHNESS	61
3.4 : DAMAGE ZONE	61
3.5 : STACKING SEQUENCE	61
3.6 : CONCLUSIONS	64
3.7 : SCOPE FOR FURTHER WORK	65

LIST OF FIGURES

Fig. No.	Title	Page No.
1.1	Crack tip coordinate system and arbitrary line integral contour	6
1.2	A cracked body with constant	9
	(a) Load applied	
	(b) Displacement applied	
1.3	Generalized load deflection dia- gram with prescribed load	10
1.4	Generalized load deflection diagram with prescribed displacement	12
1.5	Analysis procedure for method 4[17]	17
2.1	Longitudinal stress-strain curve for Quasi-isotropic laminate	20
2.2	Transverse stress-strain curve for Quasi-isotropic laminate	21
2.3	Longitudinal stress-strain behaviour of cross-ply laminate	22
2.4	Transverse stress-strain behaviour of cross-ply laminates	23
2.5	Specimen configuration	25
2.6	Experimental arrangement for cutting notches	26
2.7	Experimental arrangement on MTS machine	27

Fig. No.	Title	Page No.
3.1	Load displacement record for $[0/\pm 45/90]_{2s}$ glass fibre reinforced epoxy laminate	30
3.2	Load displacement record for $[90/\mp 45/0]_{2s}$ glass fibre reinforced epoxy laminate	31
3.3	Transmitted light photograph of two specimens of $[0/\pm 45/90]_{2s}$ configuration with different crack lengths	33
3.4	Variation of critical displacement with crack length for two different configurations	35
3.5	Variation of strain energy per unit thickness with dis- placement for two different configurations	37
3.6	J-integral as a function of dis- placement for two different configurations	38
3.7	Load displacement record for $[0/\pm 45/90]_{2s}$ GFRP with $l=75$ mm	41
3.8	Load vs displacement curve for $[0/\pm 45/90]_{2s}$ and $l = 150$ mm.	42
3.9	Variation of critical displace- ment with specimen length for $[0/\pm 45/90]_{2s}$ GFRP.	43

Fig. No.	Title	Page No.
3.10	Variation of strain energy with specimen length for different initial crack lengths for $[0/\pm 45/90]_{2s}$ GFRP.	45
3.11	Strain energy at the crack tip for different initial crack lengths for $[0/\pm 45/90]_{2s}$ GFRP	47
3.12	Load displacement record for $[0/90]_{4s}$ glass fibre reinforced epoxy laminate	48
3.13	Variation of critical displacement with crack length for $[0/90]_{4s}$ GFRP.	50
3.14	Variation of strain energy per unit thickness with displacement for cross-ply laminate	51
3.15	J-integral as a function of displacement for $[0/90]_{4s}$ GFRP.	52
3.16	Load displacement behaviour for $[0/90]_{4s}$ GFRP with $l = 75$ mm	53
3.17	Load displacement behaviour for $[0/90]_{4s}$ GFRP with $l = 125$ mm	54
3.18	Variation of critical displacement with crack length for $[0/90]_{4s}$ GFRP with $l = 75$ mm	55
3.19	Variation of critical displacement with crack length for $[0/90]_{4s}$ GFRP with $l = 125$ mm	56

Fig. No	Title	Page no.
3.20	Variation of critical displacement with specimen length for $[0/90]_{4s}$ GFRP.	58
3.21	Variation of strain energy with specimen length for different initial crack lengths for $[0/90]_{4s}$ GFRP.	59
3.22	Variation of strain energy at crack tip for different initial crack lengths for $[0/90]_{4s}$ GFRP	60
3.23	Transmitted light photograph of two specimens of $[0/90]_{4s}$ configuration with different crack lengths.	62

NOMENCLATURE

A	Area
a	Crack length
COD	Crack mouth opening displacement
d	Generalised displacements
F	Generalised force
G	Energy release rate
J	J-integral
J_{1c}	Critical value of J-integral in mode I
LEFM	Linear elastic fracture mechanics
l	Length of the specimen
P	Load
r	Near tip crack field length parameter
S	Boundary of a two dimensional body
S_T	Portion of boundary where traction is prescribed
SEN	Single edge notched specimen
T_i	Traction vector
t	Thickness
U	Potential energy per unit thickness
u_i	Displacement vector
v_f	Fibre volume fraction
W	Strain energy density function

(x₁)

w Width

x₁ , x₂ Coordinates

σ Stress along load direction

σ_{ij} Stress tensor

ϵ Strain along load direction

δ Crack mouth opening displacement

Γ J-integral contour

ν Poisson's ratio

ABSTRACT

Fracture toughness of Quasi-isotropic and cross-plied laminates has been investigated experimentally. The present studies were performed on glass fibre reinforced epoxy laminates supplied by the 3M Company of U.S.A. The testing was conducted on SEN specimens in a 10 Ton MTS machine under stroke control. Instantaneous values of load, load point displacements were recorded through a X-Y recorder. The data was analysed through J-integral approach.

Composites, in general do not exhibit self-similar crack extension. Instead a damage zone is formed. Damage zone is a region of stable crack growth at the crack tip. In such a case, characterization of the crack tip by a parameter calculated without focussing attention directly at the crack tip would provide an easier method of analysing fracture. The J-integral proposed by Rice is such a parameter. Its value depends on the near tip stress strain field. However, the path independent nature of the integral allows an integration path taken sufficiently far from the crack tip to be substituted for a path close to the crack tip region.

The critical value of J-integral (J_{1c}) is found out to be independent of crack length when a/W is greater than (i) 0.5 for Quasi-isotropic laminates and (ii) 0.4 for cross-ply laminates. For lower crack lengths the general material damage away from the crack tip also influences the energy absorbed. However, through an extrapolation method which has earlier been proposed, the crack tip energy has been separated from the energy absorbed due to general material damage.

J_{1c} thus obtained for a/W (i) < 0.5 for Quasi-isotropic laminates and (ii) < 0.4 for cross-ply laminates are independent of crack length and its value is nearly the same as that obtained without extrapolation. Size of the damage zone, stacking sequence have been found to affect the fracture toughness of the material.

CHAPTER I

INTRODUCTION

1.1 COMPOSITES

Composite materials, as the name suggests are a combination of two or more distinct materials so as to achieve certain physical properties not realizable individually. Their light weight and high specific strength yield them as useful structural material in space vehicles. In addition they also posses useful properties such as high stiffness, toughness, vibration, fatigue and corrosion resistance and high temperature performance. Although significant weight savings, paramount in transportation engineering, are possible, composites have gone far beyond being simply lighter than conventional materials. They offer real structural advantages with almost unbounded potential. The ability to tailor a particular matrix material to suit prevailing environmental conditions whilst maintaining adequate reinforcement to withstand applied loading is unquestionably an attractive proposition.

1.2 FRACTURE MECHANICS OF COMPOSITES

Stress analysis techniques based on effective moduli or other continuum mechanics approaches to fibre/matrix laminates have provided rules for selecting lay up angles and laminate geometries to obtain specified stiffness. However, few rules exist which have a basis in a failure analysis. If composites are to be used to their fullest extent as engineering materials, it will be necessary to know in advance their limits in load-bearing applications. To do this, predictive techniques for the various failure modes that can occur in such applications must be established. Fracture mechanics, the discipline concerned with failure by crack initiation and propagation, is a natural tool to use for this purpose.

Fracture of composites is highly complex in nature involving any one or a combination of the following: breaking of the fibres, fibre pull out, debonding between the fibres and matrix, matrix cracking etc. The problem of characterising fracture behaviour of composite materials is challenging as the crack propagation in them differ substantially from the cracks in homogeneous isotropic materials which exhibit self-similar crack growth. The additional complexities in composites underscore the need for parallel or combined experimental

and theoretical analyses. Fracture mechanics of composite materials, together with its initiation, propagation and controlling parameters, represents a significant problem.

Fracture toughness of a material represents its resistance to crack initiation and propagation. There are different methods and procedures to obtain fracture toughness namely the R-curve approach and the J-integral approach. The R-curve approach has been studied more widely for metallic materials and has been extended to composites [1-4] in the last decade. Investigators have considered the damage zone as a self-similar crack extension. The instantaneous crack length is estimated by a compliance matching procedure. This approach is somewhat lengthy and consumes time.

As stated earlier composites, in general, do not exhibit self-similar crack extension. Instead a damage zone is formed. Damage zone is a region of stable crack growth at the crack tip. In such a case characterization of the crack tip by a parameter calculated without focussing attention directly at the crack tip would provide an easier method of analysing fracture. The J-integral proposed by Rice [5] is such a parameter. Its value depends on the near tip stress strain field.

However, the path independent nature of the integral allows an integration path taken sufficiently far from the crack tip to be substituted for a path close to the crack tip region. The basis for J-integral is provided by the works of Rice and Rosengren [7] and Hutchinson [6]. They have shown that a singularity in the stress and strain does exist at the crack tip which is uniquely dependent upon the material flow properties. Mc Clintock [8] has demonstrated that the crack tip stress and strain field can be described in terms of J-integral. The use of J-integral as an elastic plastic criterion has been discussed by Broberg [9] from an analytical standpoint. Begley and Landes [10-12] through extensive experiments have shown the applicability of J-integral as a fracture criterion for metals.

It is well known that in composite materials, microcracks at fibre matrix interface appear at very low loads due to the stress concentrations produced by the fibres lying perpendicular to the load. It is probably this unavoidability of microcracks that has deterred the researchers from exploring the applicability of the J-integral as a fracture criterion for composite materials. Recently Agarwal, Patro and Kumar [13] have developed J-integral as a fracture criterion for short fibre composites. They have evaluated J-integral using an energy

rate interpretation. The present work proposes to extend the J-integral method to the oriented fibre composites.

1.3 BASIS FOR J-INTEGRAL

The J-Integral as proposed by Rice [5], is a two dimensional energy line integral

$$J = \oint_{\Gamma} (W dx_2 - T_i \frac{\partial u_i}{\partial x_1} ds) \quad (1.1)$$

where Γ is any contour traversing in a counter clockwise sense and enclosing the crack tip as shown in Fig. 1.1. The components of traction vector are $T_i = \sigma_{ij} n_j$ where σ_{ij} is the stress tensor and n_j normal vector to Γ ; u_i is the displacement vector and s the arc length along Γ . W , the strain energy density, is defined as

$$W = W(\epsilon_{mn}) = \int_{\Omega} \sigma_{ij} d\epsilon_{ij} \quad (1.2)$$

where ϵ_{ij} is the strain tensor.

The J-integral characterizes the crack tip field, the basis of which is provided by the works of Hutchinson [6] and Rice and Rosengren [7]. They have extended fracture mechanics concepts to cases of large scale yielding which also assumes the existence of a crack tip singularity. They indicate that the product of plastic stress and strain approaches a $1/r$ singularity; r being a near tip crack field length parameter. The crack tip singularity is uniquely dependent on the material constitutive

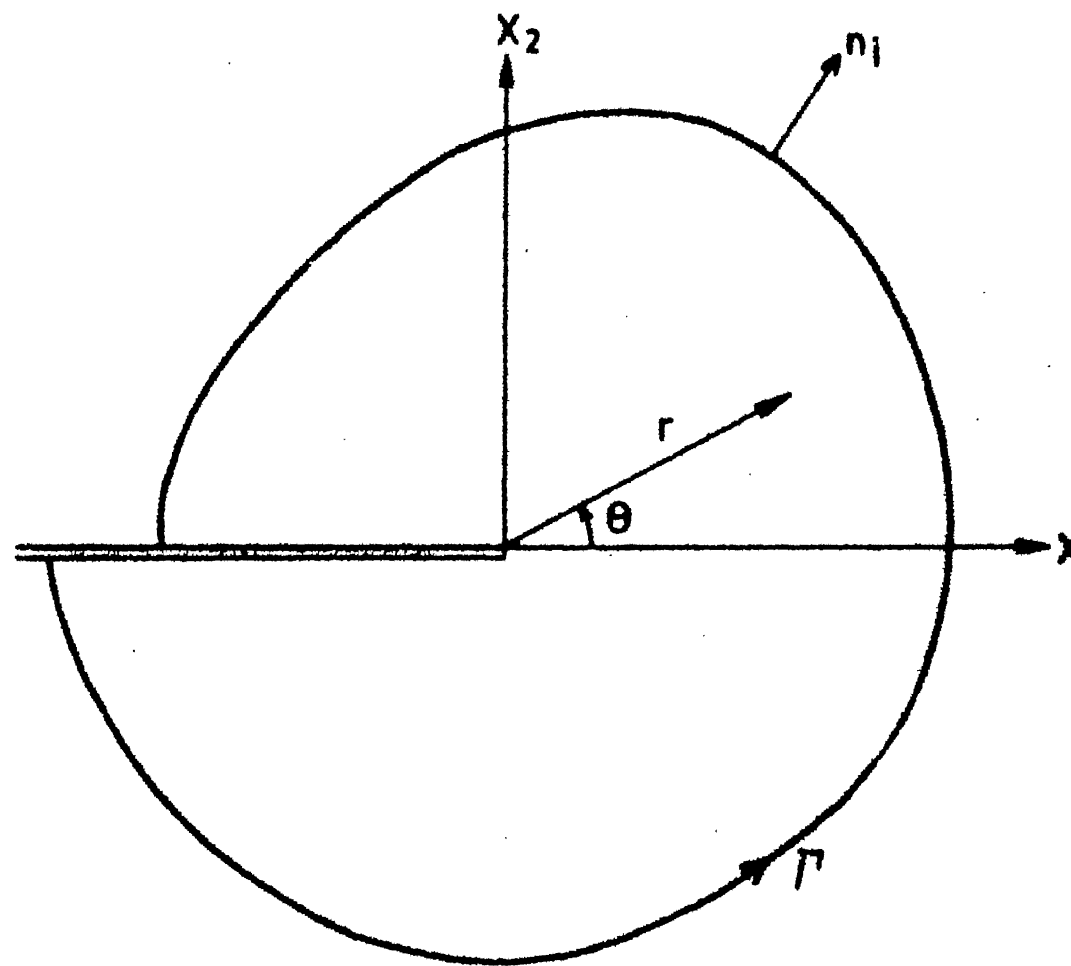


Fig. 1.1 Crack tip coordinate system and arbitrary line integral contour.

relations. For a deformation theory of plasticity, Mc Clintock [8] has demonstrated, through the crack tip plastic stress and strain equations expressed from the Hutchinson Rice Rosengren (HRR) singularity, the existence of a singularity in r whose strength is J-integral.

The J-integral has another important advantage as a fracture criterion. Broberg [9] considered crack growth criteria for a nonlinear elastic body containing a crack. For such a body, stress and strain singularities occur at the crack tip. This region ahead of the crack tip is termed as the end region outside which the material may be regarded as a continuum. As the load is increased, the end region eventually reaches a critical state at which the crack starts moving. One prominent feature of the end region at critical state is that the state is neither dependent on the distribution of loads nor on the crack length. It simply and solely depends on the material itself. The end region can be specified by J-integral. Also, J-integral reaches a critical value, J_c , as the end region reaches the critical state.

From the foregoing discussion, it is evident that J-integral displays three prominent features attractive to its use as a fracture criterion namely,

(i) J-integral as a field parameter indicates the stress and strain distribution in a cracked body.

(ii) It describes the crack tip region by specifying the strength of the singularity.

(iii) Critical value of J-integral, J_c is a material property which can be used as a fracture criterion when unstable crack growth occurs.

The J-integral can be conveniently evaluated experimentally through its energy rate interpretation. It may be noted that in Eq. 1.1 the two terms in the integrand namely W and $T_i \frac{\partial u_i}{\partial x_1}$, have the dimensions of energy. Thus, J is an energy related quantity. In fact Rice [5] has shown that the J-integral is equal to the change in potential energy for a virtual crack extension

$$J = - \frac{\partial U}{\partial a} \quad (1.3)$$

where U is the potential energy per unit thickness. For a two dimensional elastic body of area A , with a boundary s , the potential energy is given by

$$U = \int_A W \, dx_1 \, dx_2 - \int_{S_T} T_i u_i \, ds \quad (1.4)$$

where S_T is the portion of the boundary over which traction, T_i is prescribed. A cracked body with prescribed boundary conditions is shown in Fig. 1.2. If the boundary conditions are given in terms of the generalised force, F , the potential energy is represented by the shaded area above the load displacement curve in

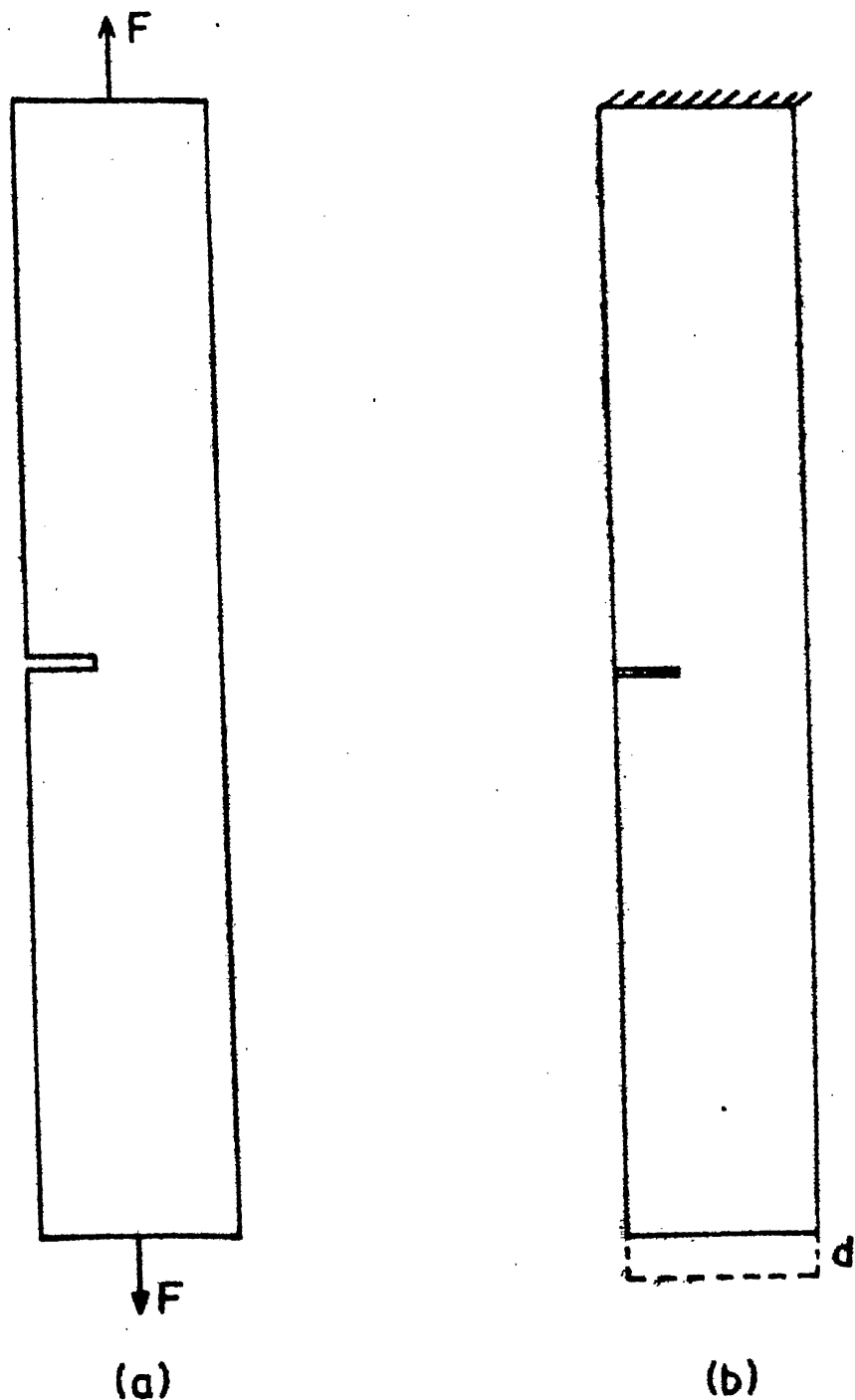


Fig. 1.2 A cracked body with constant
(a) load applied
(b) displacement applied

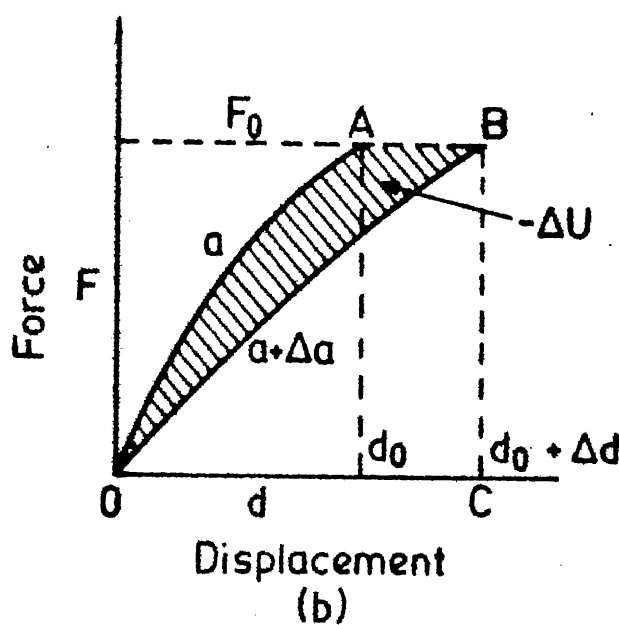
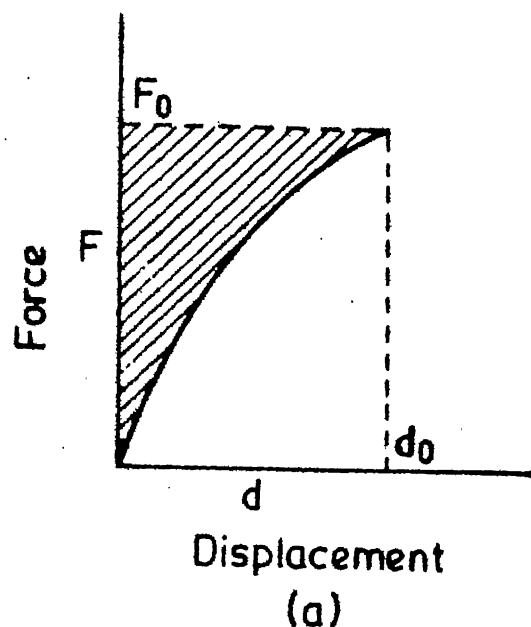


Fig. 1.3 Generalized load deflection diagram with prescribed load.

Fig. 1.3a. In this instance the potential energy is negative and its magnitude is equal to the complementary energy [10]. When the boundary conditions are prescribed in terms of generalised displacements the second term in Eq. 1.4 drops out since the traction \bar{T} on it is zero most of the time. The potential energy is then equal to the strain energy or the area under load deflection curve in Fig. 1.4a.

The J-integral can be evaluated considering the load deflection diagrams of similar bodies with neighbouring crack sizes. When two similar bodies with crack lengths a and $a + \Delta a$, are loaded, the load deflection curves are represented by OA and OB. If in the first body, the crack extends from a to $a + \Delta a$ under prescribed load, F_o , the total work done on the body is represented by the area OABCO (Fig. 1.3b). Because of reversibility, the unloading curve from the point B is the same as the loading curve of the body starting with a crack length, $a + \Delta a$. The strain energy of the body with a crack length, $a + \Delta a$, under the load F_o is the area OBCO. The shaded area OABO ($-\Delta U$) is the energy available for crack extension. Similarly when the crack extends from a to $a + \Delta a$, under prescribed displacements, the energy available for crack extension is the shaded area OABO (Fig. 1.4b). It may be mentioned that the difference in energy obtained

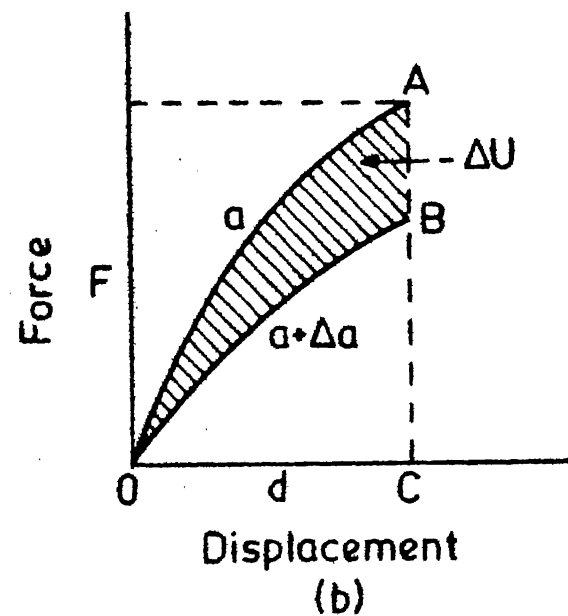
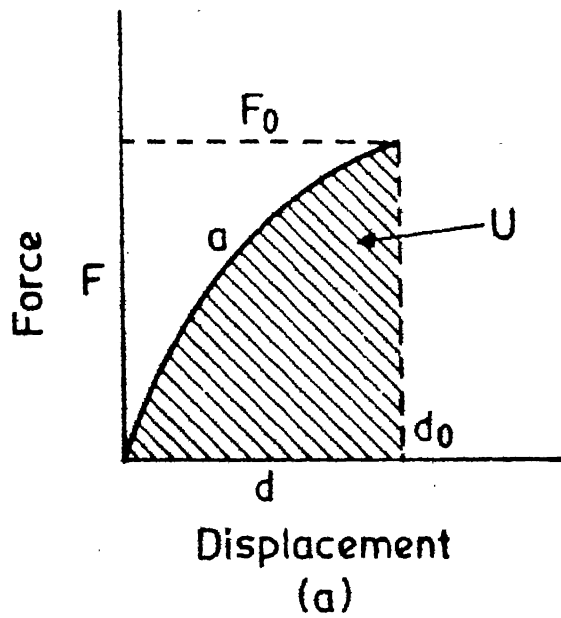


Fig. 1.4 Generalized load deflection diagram with prescribed displacement.

by the two methods is of the second order. However for an experimental evaluation of J-integral, the prescribed displacement boundary condition is preferable since, for two specimens of neighbouring crack sizes, the displacements at fracture are observed to be nearly equal, whereas the fracture loads are found to be quite different. Furthermore, for higher crack length specimens, at which J-integral is evaluated, the load-deflection diagrams become flat and it is more appropriate to evaluate J in terms of displacement. In such a case, Eq 1.3 can be written as

$$J = - \left. \frac{\partial U}{\partial a} \right|_{\text{constant displacement}} \quad (1.5)$$

Begley and Landes [10-12] have used the above relation to evaluate J-integral as a fracture criterion for metals. They demonstrated the applicability of J-integral for the case of large scale yielding at the crack tip through experimental results on an intermediate strength rotor steel. They observed that the J-integral at failure for fully plastic behaviour was equal to the linear elastic value of strain energy release rate (G) at failure for extremely large size specimens. Thus, the J-integral approach eliminates the necessity of testing very large specimens. In the present study J-integral approach is extended to oriented fibre composites.

1.4 J-INTEGRAL ESTIMATION PROCEDURES

A very good summary and comparison of J estimation procedures has been given by Chipperfield [14]. He has given as many as 9 methods and compared their relative merits.

In Method 1, use is made of the eqn. 1.5,

$$J = - \frac{\partial U}{\partial a} \quad \left| \begin{array}{l} \\ \text{constant displacement} \end{array} \right. \quad (1.5)$$

to evaluate J experimentally by using a series of specimens with different initial crack lengths. This multi-specimen evaluation procedure is clearly expensive and tedious. However, it is considered to represent the method with which the other analyses should be compared in any assessment of relative accuracy. This method has been used in the present study.

The second method is a numerical technique broadly similar to the method 1 and has been advocated by Bucci [15]. This method makes use of the equation,

$$J = - 1/B \left[\frac{\partial}{\partial a} \left(\int P d\Delta \right) \right]_{\Delta} \quad (1.6)$$

where P is the load, Δ the displacement and B the thickness of the specimen. Here plastic zone correction, slipline field predictions are made use of. This technique requires only the measurement of Δ during the fracture toughness test although the yield stress σ_y .

the ultimate tensile strength σ_u , the young's modulus E of the test material are also required. However this technique is not used for composite materials.

In the third method, the following relationship originally proposed by Rice, Paris, Merkle [16] has been used:

$$J = 2 U_c / B(w-a) \quad (1.7)$$

Here U is the energy absorbed by specimen in bending, w , the width and a , the crack length. The term U_c is obtained from U after subtracting the extraneous energy components arising from load point indentations and testing machine compliance effects. This technique when applied to composites leads to energy dissipation due to load point indentation which cannot be estimated accurately. Also the thin composite specimens slip off when load is applied and hence this technique is not used for composites.

A more general version of the above method is due to Sumpter and Turner [17] for three point bend compact tension tests. Here J is separated into that due to elastic and plastic effects as,

$$J = J_e + J_p \quad (1.8)$$

$$= [\eta_e U_e / (w-a) B] + [\eta_p U_p / (w-a) B]$$

where η_p is usually assumed as 2 and η_e is obtained from tables corresponding to the type of specimen and a/W ratio. The areas U_e and U_p are found from the graph as depicted in Fig. 1.5. This is also not used often for composites because of the problems mentioned earlier.

The rest of the methods are slight modifications of the method 4 [17] and hence not used often in the case of composites.

Bamford and Bush [18] have carried out experiments to characterize fracture behaviour of stainless steel using J-integral approach. For monitoring crack extension they have used different techniques including unloading compliance, electrical potential, acoustic emission inaddition to the multi-specimen heat tinting method used for baseline data. The heat tinting method although quite popular among metals, cannot be applied to composites. Electric potential technique can be applied only for Carbon Fibre Composites (CFRP) and it does not work for GFRP. Acoustic Emission technique can be applied to composites.

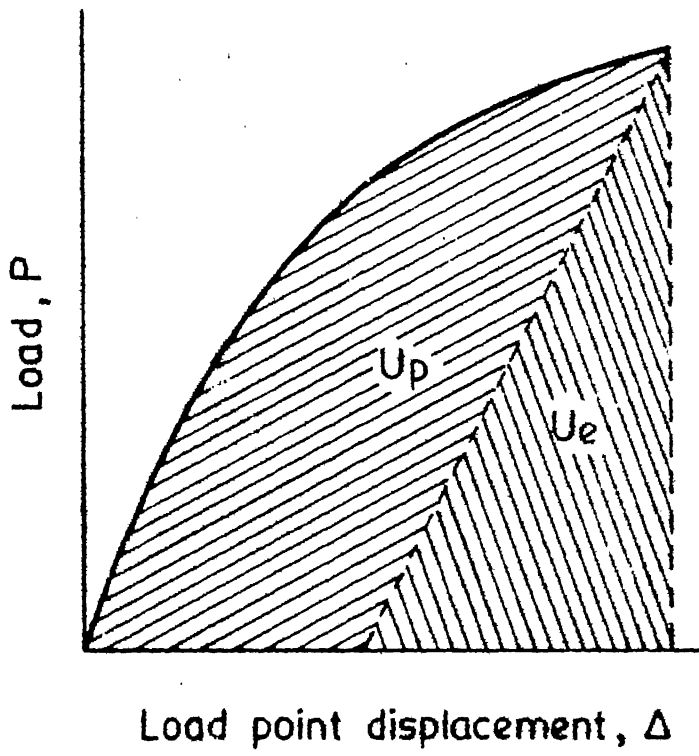


Fig. 1.5 Analysis procedure for method 4. [17]

1.5 SCOPE OF THE PRESENT WORK

The current studies are an attempt to characterize fracture behaviour of composite materials. Researchers are far from agreeing on applicability of a particular fracture mechanics principle to composite materials. The opinion is so widely varying on the topic that some authors even wonder if the concepts of LEFM can be extended to composites at all. Recently Patro [20] has applied J-integral technique to short fibre composites. The current studies are an extension of the above principle to oriented fibre composites. Quasi-isotropic and cross-plyed laminates have been tested. These are often used as structural material and hence studied.

CHAPTER II

EXPERIMENTAL DETAILS

The present studies were performed on glass fibre reinforced epoxy laminates supplied by the 3M Company of U.S.A. Short fibre composites which are isotropic in the plane have earlier been analysed. As a next step the quasi-isotropic laminates of configurations $[0/\pm 45/90]_{2s}$ and $[90/\pm 45/0]_{2s}$ were studied. Crossply laminates of $[0/90]_{4s}$ configuration have also been tested. The stress-strain behaviour of the laminates are shown in Figs. 2.1 to 2.4. Their properties are summarised below:-

	<u>Quasi-isotropic laminate</u>	<u>Cross-ply laminate</u>
Volume fraction of fibres, v_f	46.5%	43.5%
Moduli of elasticity		
Longitudinal, E_L	18.82 GPa	20 GPa
Transverse, E_T	30 GPa	8.0 GPa
Ultimate tensile strength		
Longitudinal, σ_{LU}	240 MPa	405 MPa
Transverse, σ_{TU}	240 MPa	325 MPa

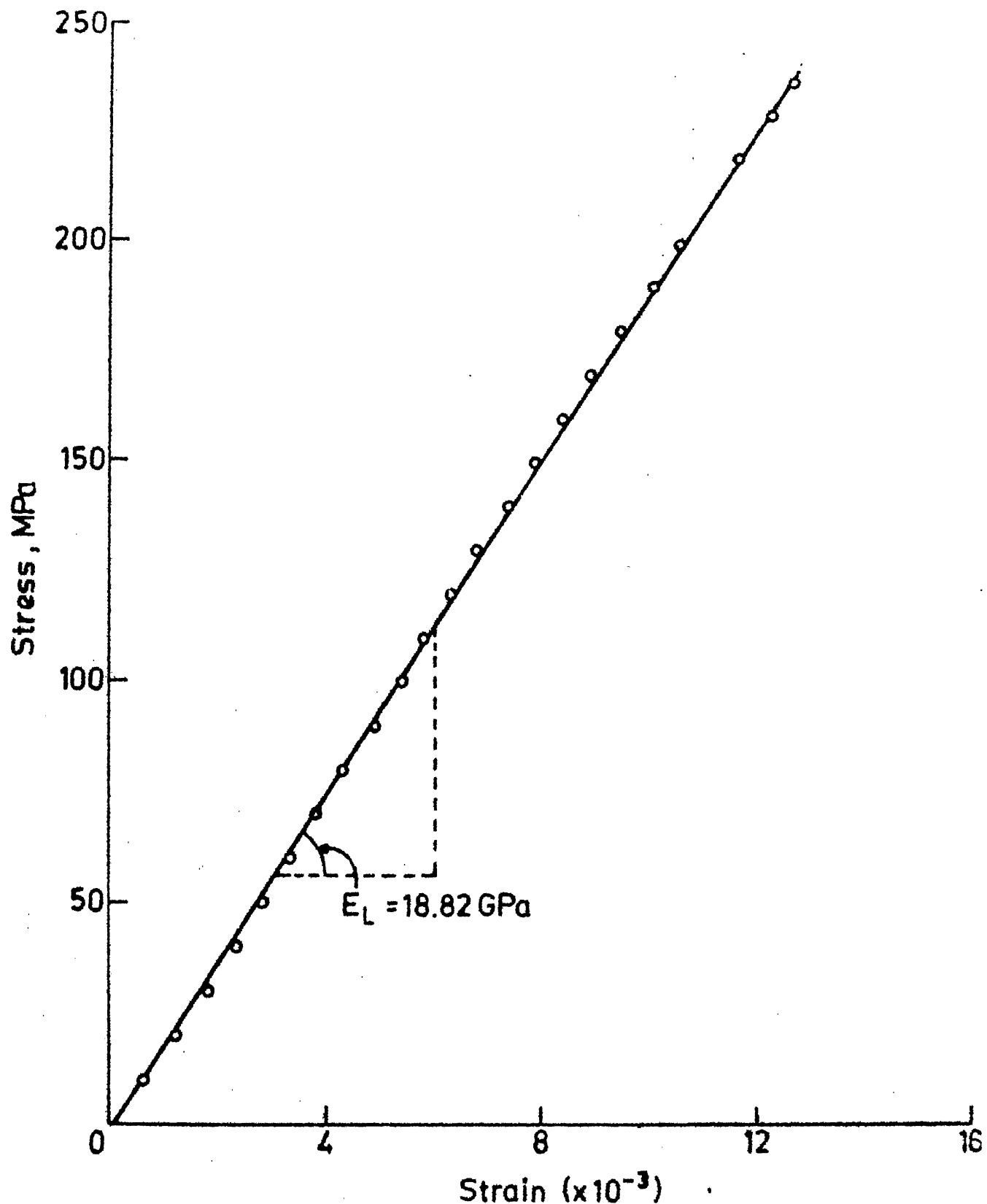


Fig. 2.1 Longitudinal stress-strain curve for Quasi-isotropic laminate.

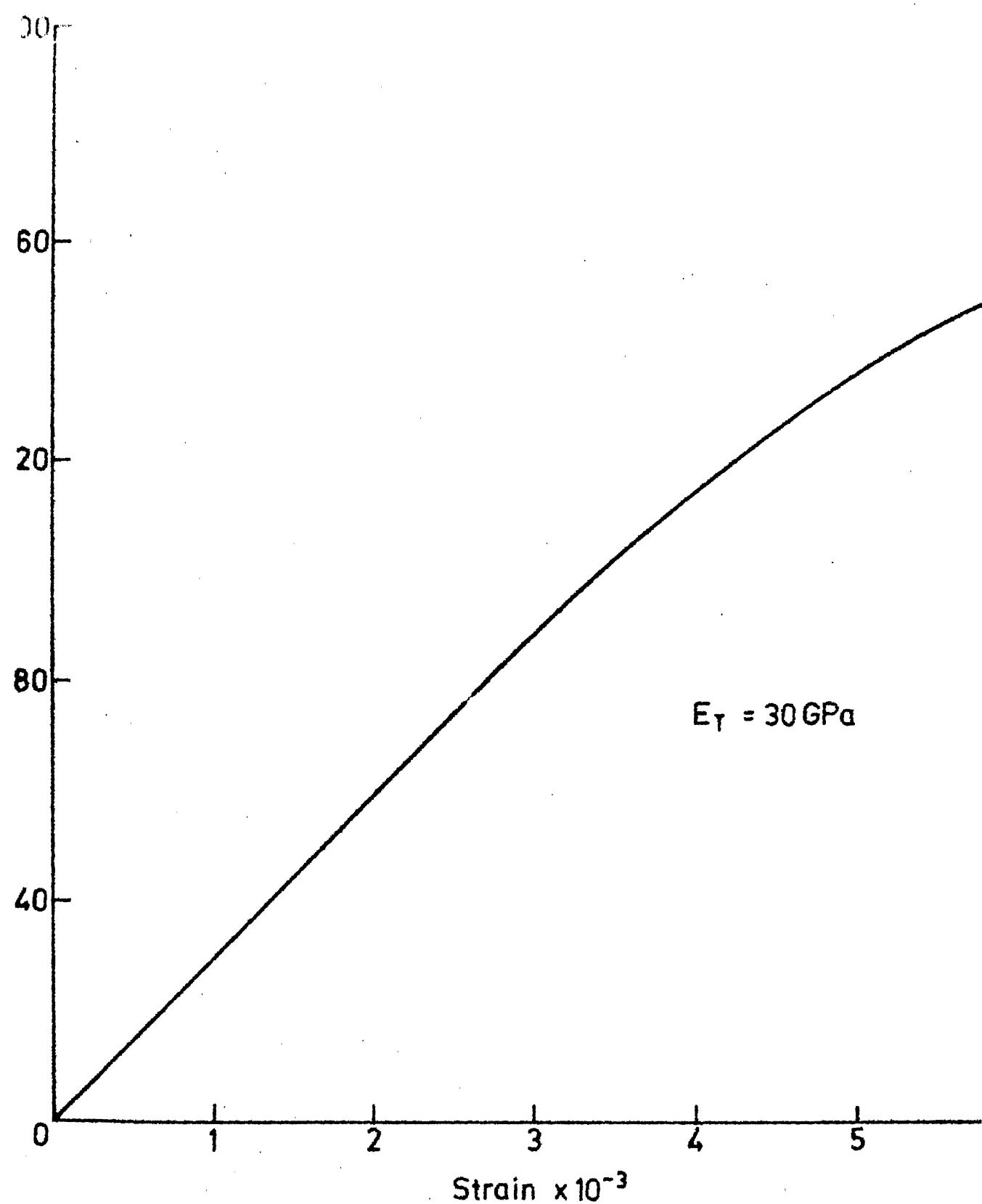


Fig. 2.2 Transverse stress-strain curve for Quasi-isotropic lamina

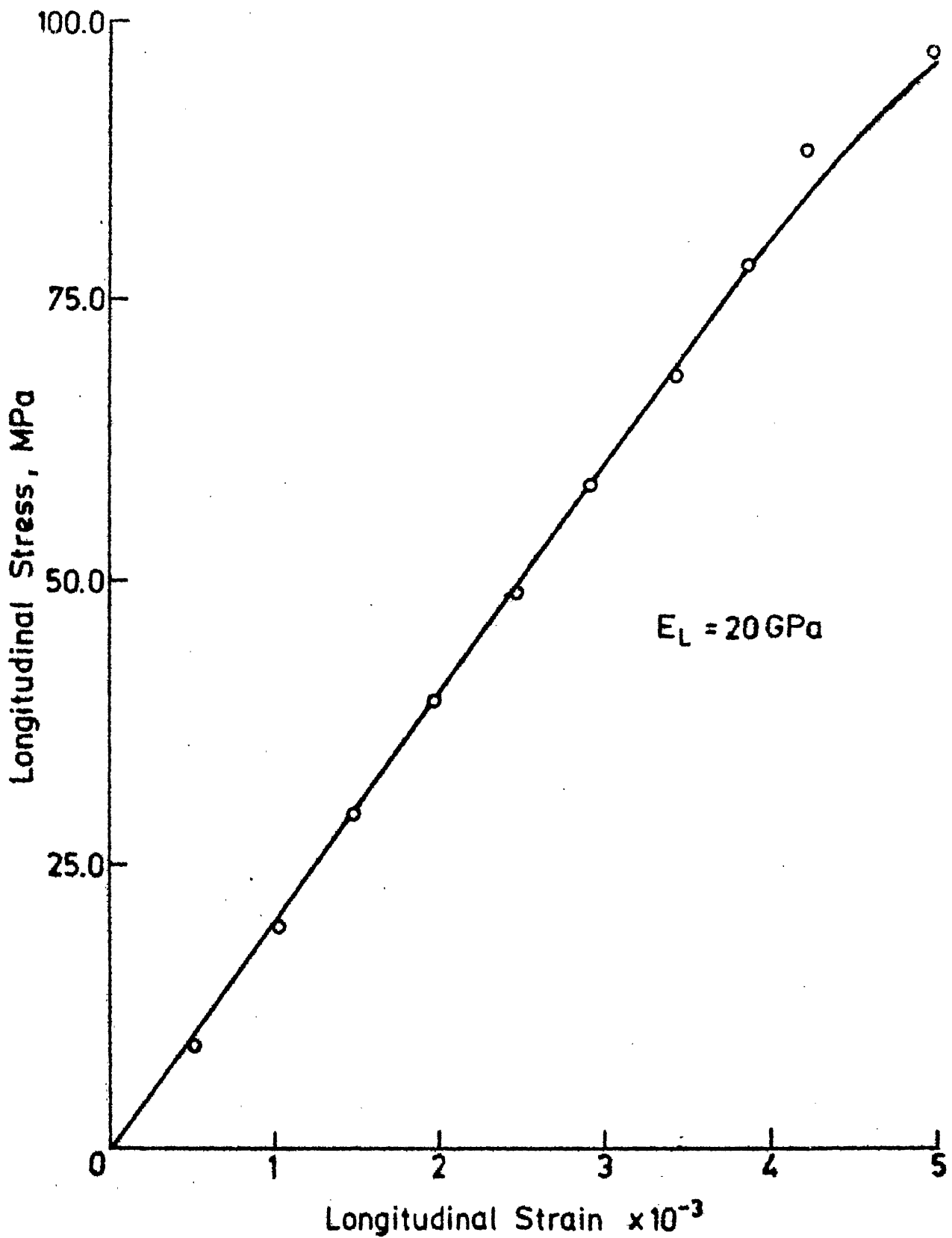


Fig. 2.3 Longitudinal stress strain behaviour of crossply lamina

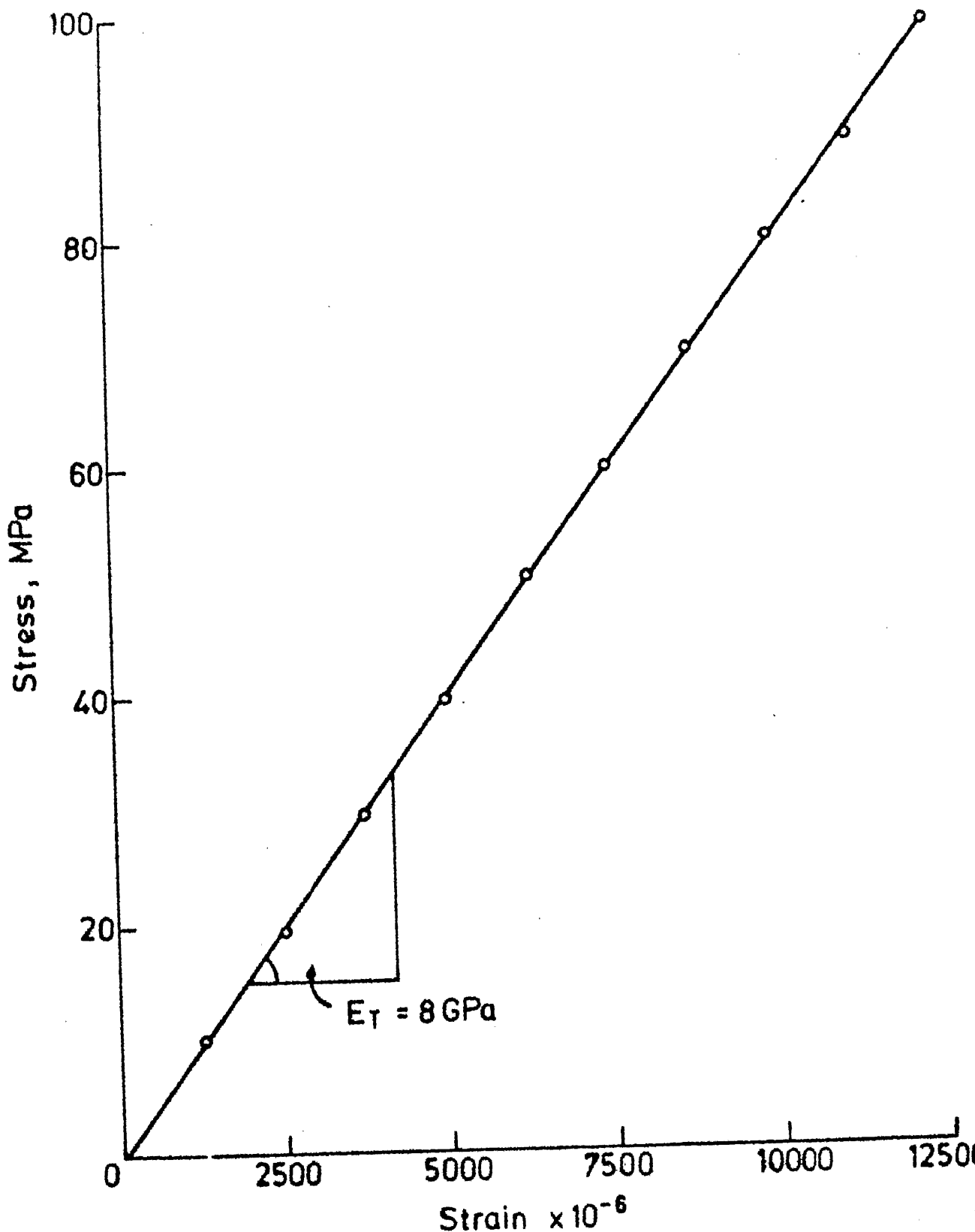


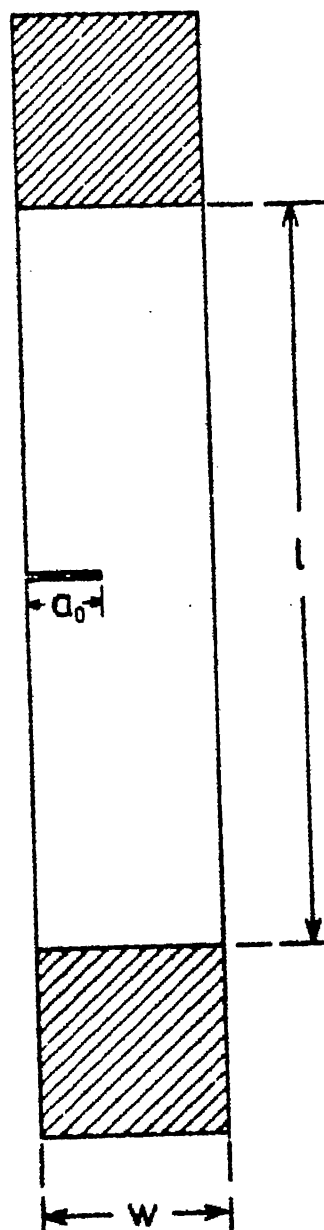
Fig. 2.4 Transverse stress strain behaviour of crossply laminates.

	<u>Quasi-isotropic laminates</u>	<u>Cross-ply laminates</u>
Poisson's ratio		
ν_{LT}	0.054	0.26
ν_{TL}	0.087	0.104
Shear modulus		
G_{LT}	18.76 GPa	4.0 GPa

Single edge notched (SEN) specimens were 25 mm wide, 3.9 mm (for Quasi-isotropic laminates) and 4.0 mm (for Cross-ply laminates) thick and length between the grips was atleast 3 times the width of the specimen. The specimen configuration is shown in Fig. 2.5. The initial notches were machined using a 0.25 mm thick slit cutter and their length varied between 2.5 and 17.5 mm. (that is, $a/W = 0.1$ to 0.7). A lathe available in the laboratory was suitably modified for cutting notches. The experimental set up is shown in Fig. 2.6.

2.1 TESTING SYSTEM

The fracture toughness testing was conducted on SEN specimens in a 10 Ton MTS machine. The general experimental arrangement is shown in Fig. 2.7. The upper grip is fixed and the lower grip can move in a vertical direction. The tests were conducted in displacement controlled mode. Instantaneous values of



$$\frac{l}{w} > 3$$

Fig. 2.5 Specimen configuration.

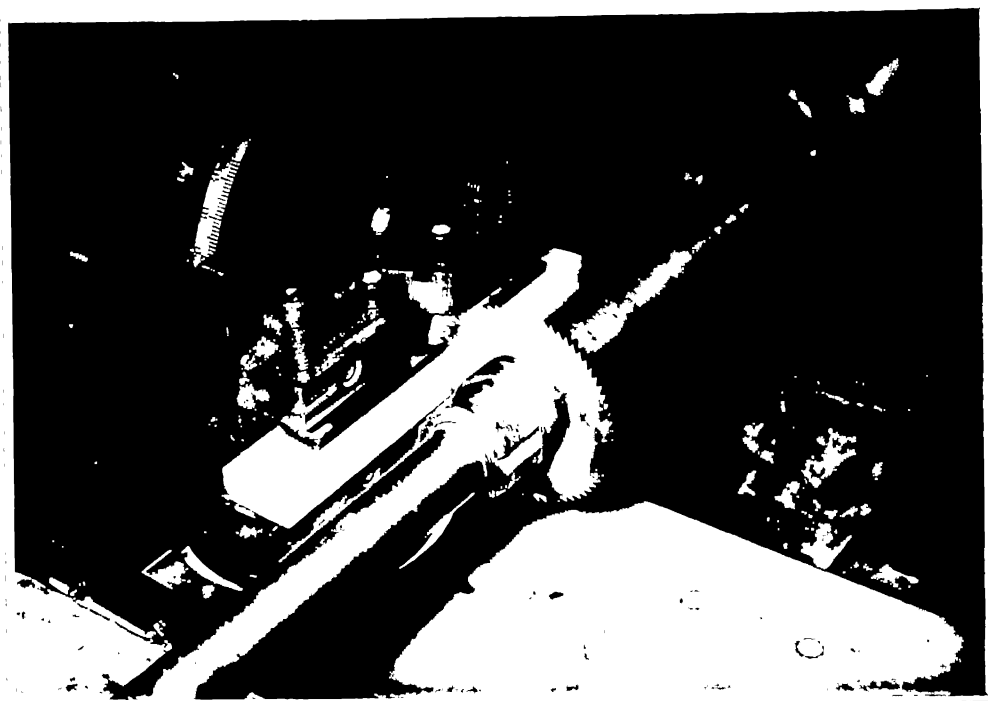


Fig. 2.6 : EXPERIMENTAL ARRANGEMENT FOR CUTTING NOTCHES

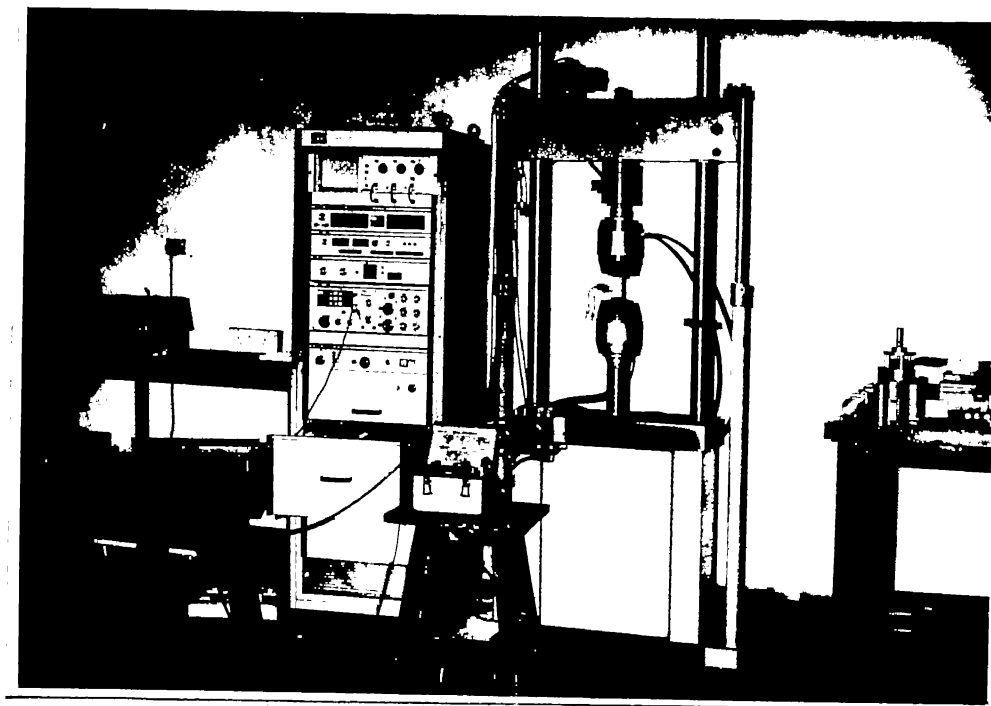


Fig. 2.7 : EXPERIMENTAL ARRANGEMENT ON MTS MACHINE

load, displacement of lower grip were recorded through a X-Y recorder. Atleast four specimens were tested for each crack length.

CHAPTER III

RESULTS AND DISCUSSION

The fracture toughness tests were conducted on (i) Quasi-isotropic laminates (two configurations) and (ii) Cross-ply laminates. The results are discussed individually in this section.

3.1 QUASI-ISOTROPIC LAMINATES

Quasi-isotropic laminates of $[0/\pm 45/90]_{2s}$ and $[90/\mp 45/0]_{2s}$ configuration have been tested under tension for fracture toughness determination. Typical load displacement (at load points) curves for specimens with different initial crack lengths are shown in Figs. 3.1 and 3.2. The tests were conducted under displacement controlled conditions so that the load displacement behaviour beyond maximum load is also clearly indicated. As the specimens were being loaded they were continuously observed under transmitted light. At low loads no damage was observed. As the load increases, damage (essentially subcracks) becomes visible at approximately 75-80% of the fracture load. Specimens containing small cracks

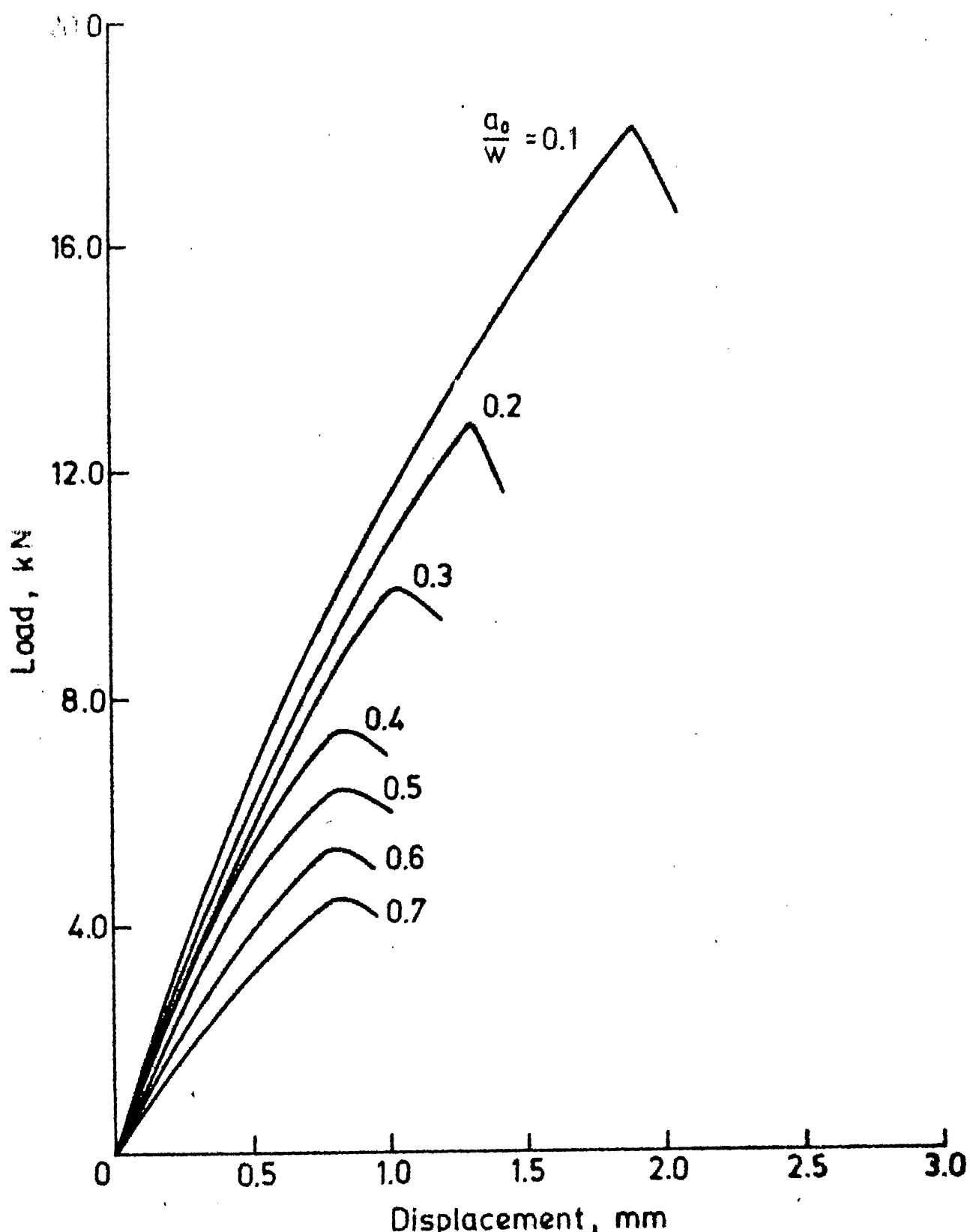


Fig. 3.1 Load Displacement record for $[0/-45/90]_{2s}$ glass fibre reinforced epoxy laminate.

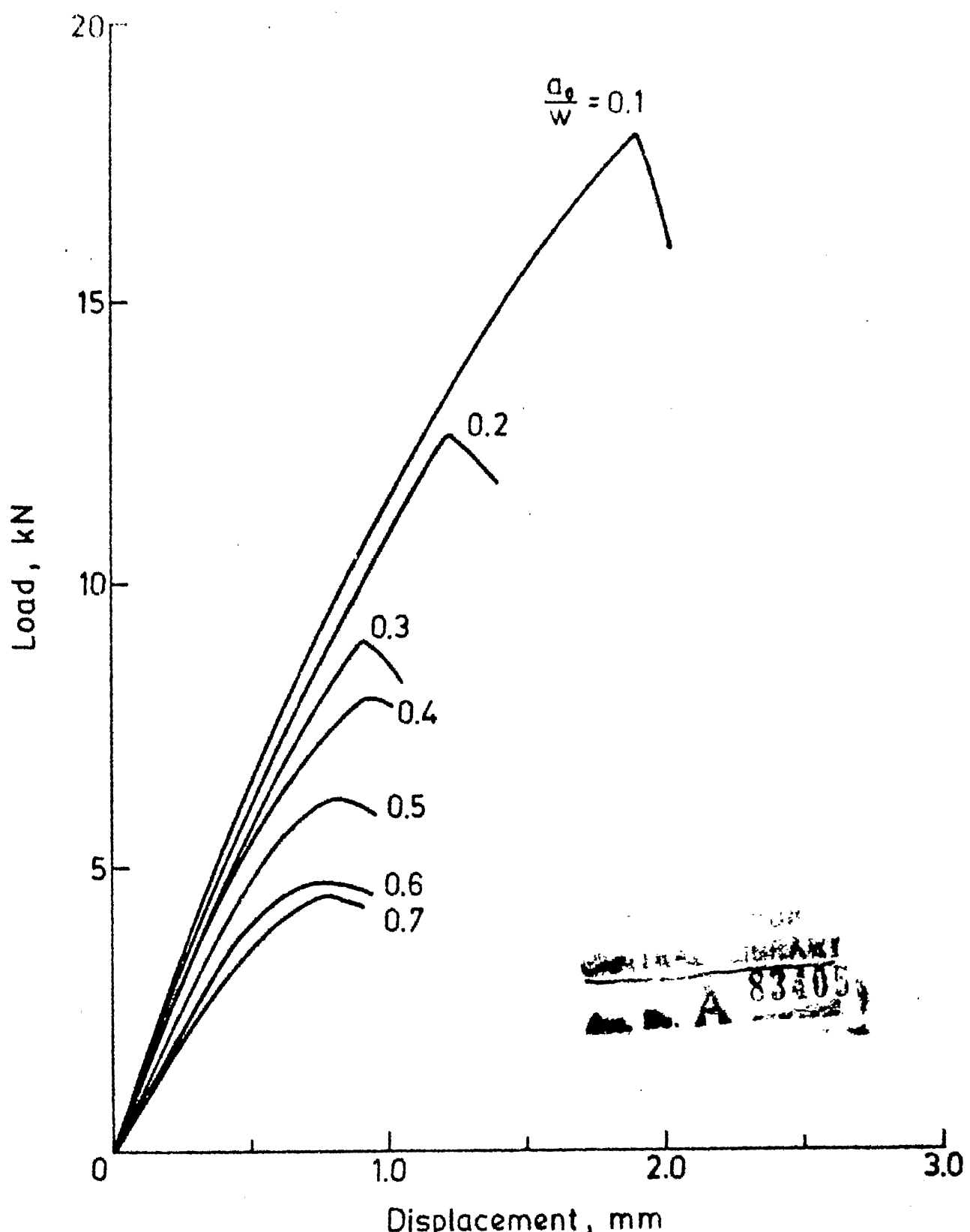


Fig. 3.2 Load displacement record for $[90/\pm 45/0]_{2s}$ glass fibre reinforced epoxy laminate.

fracture suddenly causing an abrupt drop in load whereas the specimens with larger cracks show a more gradual fracture process beyond maximum load. This behaviour is similar to that observed in metals [10] and short fibre composites [13]. This can be attributed to the fact that the strain energy stored during loading in a small crack length specimen is sufficient to cause catastrophic failure. Deeply cracked specimens do not show this trend. The photograph of two damaged specimens are shown in Fig. 3.3. The damage occurs along fibre directions in each ply and delaminations are more or less confined in a 45° triangle emanating from the crack tip. The damage zone appears more spread in the case of lower crack lengths whereas for higher crack lengths they tend to be collinear with the original crack. Recently Harris and Morris [19] studied the fracture toughness of $[0/\pm 45/90]_{ns}$ graphite/epoxy laminates as a function of specimen thickness using center cracked tension specimens. The enhanced x-ray photographs of damage zone in the $[0/\pm 45/90]_{ns}$ laminates given by them also show a similar behaviour. The size of the damage zone controls the fracture toughness of the material. This part is discussed later in this section.

The critical displacement has been defined as the displacement at which significant damage develops

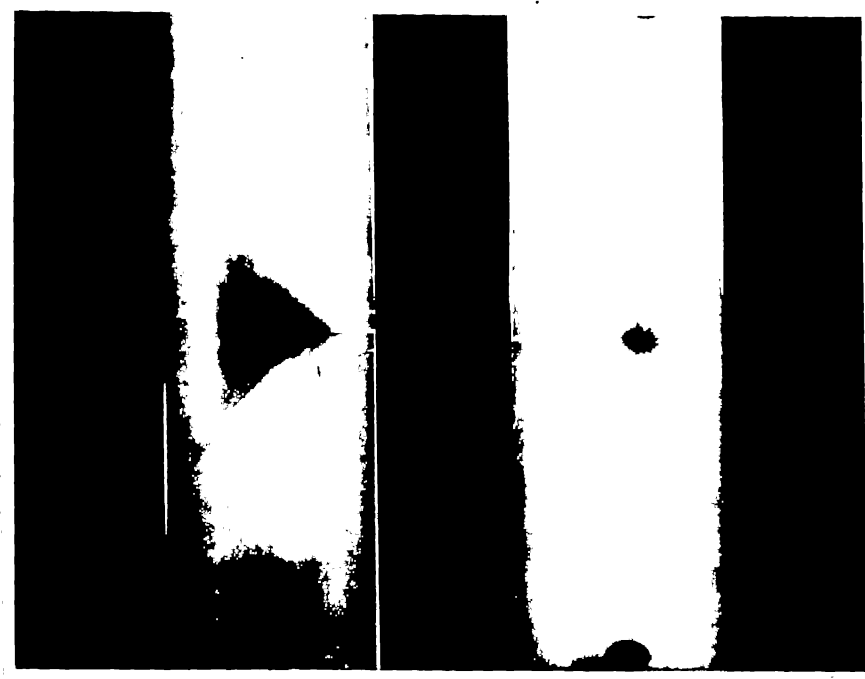


Fig. 3.3 : TRANSMITTED LIGHT PHOTOGRAPH OF TWO SPECIMENS OF $[0/ \pm 45/90]_{2s}$ CONFIGURATION WITH DIFFERENT CRACK LENGTHS.

at the crack tip and the crack starts to grow catastrophically. As has been shown by Patro [20] it coincides with that of the maximum load. In the case of small crack lengths the critical displacement decreases with increase in crack length (Fig. 3.4) whereas it remains constant for cracks larger than 12.5 mm. The initial variation in critical displacement occurs due to the significant deformations away from the crack plane because of larger loads. The constant value of critical displacement was found to be 0.75 mm for $[0/\pm 45/90]_{2s}$ and $[90/\mp 45/0]_{2s}$ laminates.

The J-integral as shown by Rice [12] can be interpreted as the difference in potential energy between two identically loaded bodies having infinitesimally differing crack lengths, da;

$$J = - \left. \frac{dU}{da} \right|_{\text{constant displacement}} \quad (3.1)$$

where U is the potential energy per unit thickness of the body and 'a' the crack length. Also when the displacement is kept constant for evaluating J the potential energy, U , reduces to the area under the load deflection record and it is equal to the strain energy [12]. Thus the area under the load displacement curves is first obtained at the intervals of 0.10 mm displacement and

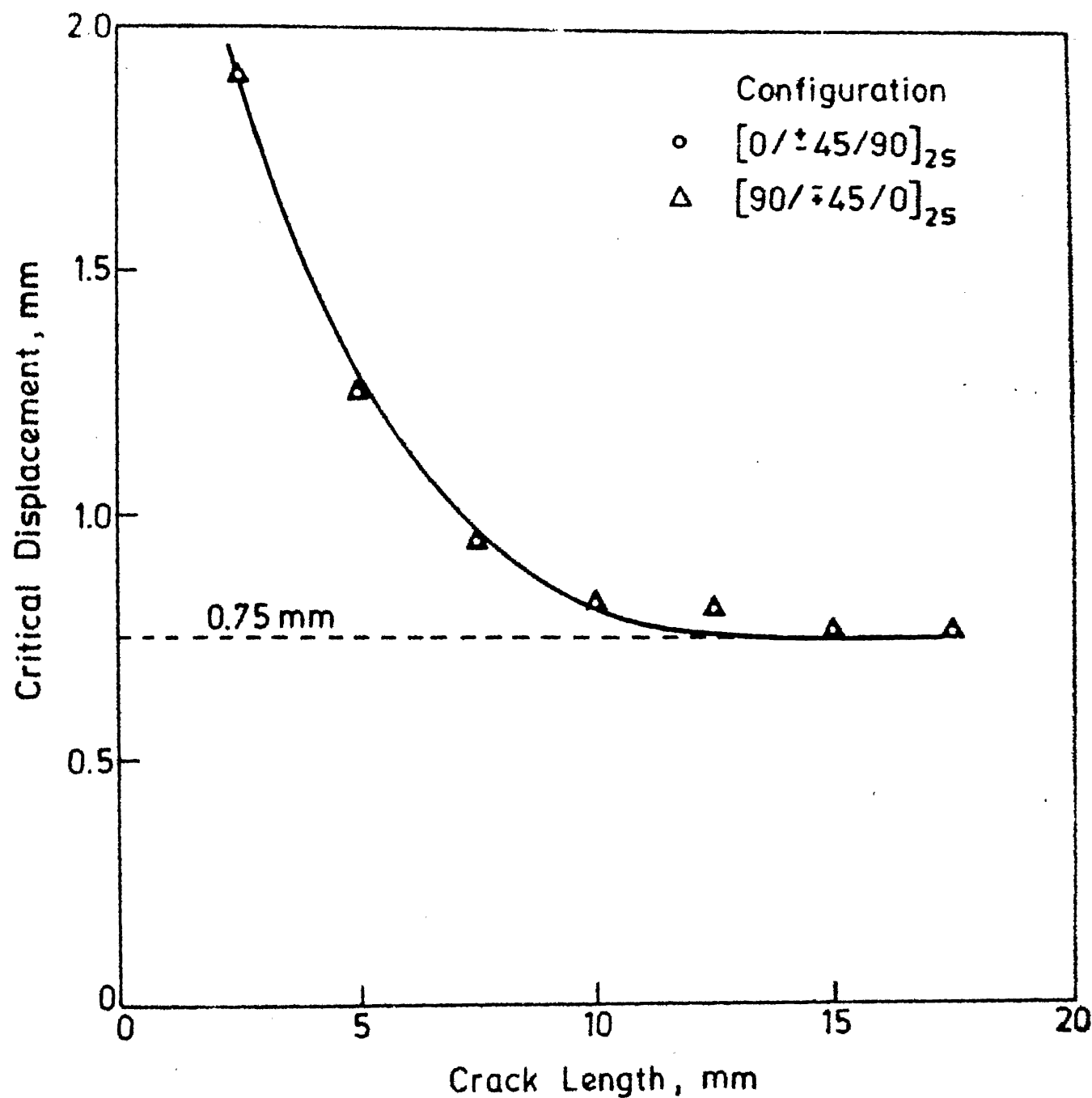


Fig. 3.4 Variation of critical displacement with crack length for two different configurations.

plotted against crack length for several displacements. (Fig. 3.5) for the two configurations. For a given displacement the energy absorbed by a specimen decreases as the crack length increases (Fig. 3.5) because smaller loads are required. The plot of energy absorbed have been approximated by two straight lines and it can be seen that the deviation is not much. For a constant displacement, the strain energy initially decreased moderately with increase in crack length and afterwards decreased more rapidly for cracks larger than 12.5 mm because in specimens with longer crack lengths the energy absorbed is essentially in the vicinity of the crack tip and is thus strongly influenced by the crack length.

The J-integral is obtained from Eq. 3.1 through the slopes of the energy curves in Fig. 3.5. With the approximation of the energy curves by two straight lines, two J-integral versus displacement plots (Fig. 3.6) for the two configurations are obtained, one for the lower ranges of crack length and the other for higher range. The critical displacement for cracks larger than 12.5 mm is 0.75 mm for both $[0/\pm 45/90]_{2s}$ and $[90/\mp 45/0]_{2s}$ configurations tested. The critical value of J-integral is found to be 46.5 kJ/m^2 for $[0/\pm 45/90]_{2s}$ configuration and 41.0 kJ/m^2 for $[90/\mp 45/0]_{2s}$ configuration. (Fig. 3.6). These values are close within the experimental

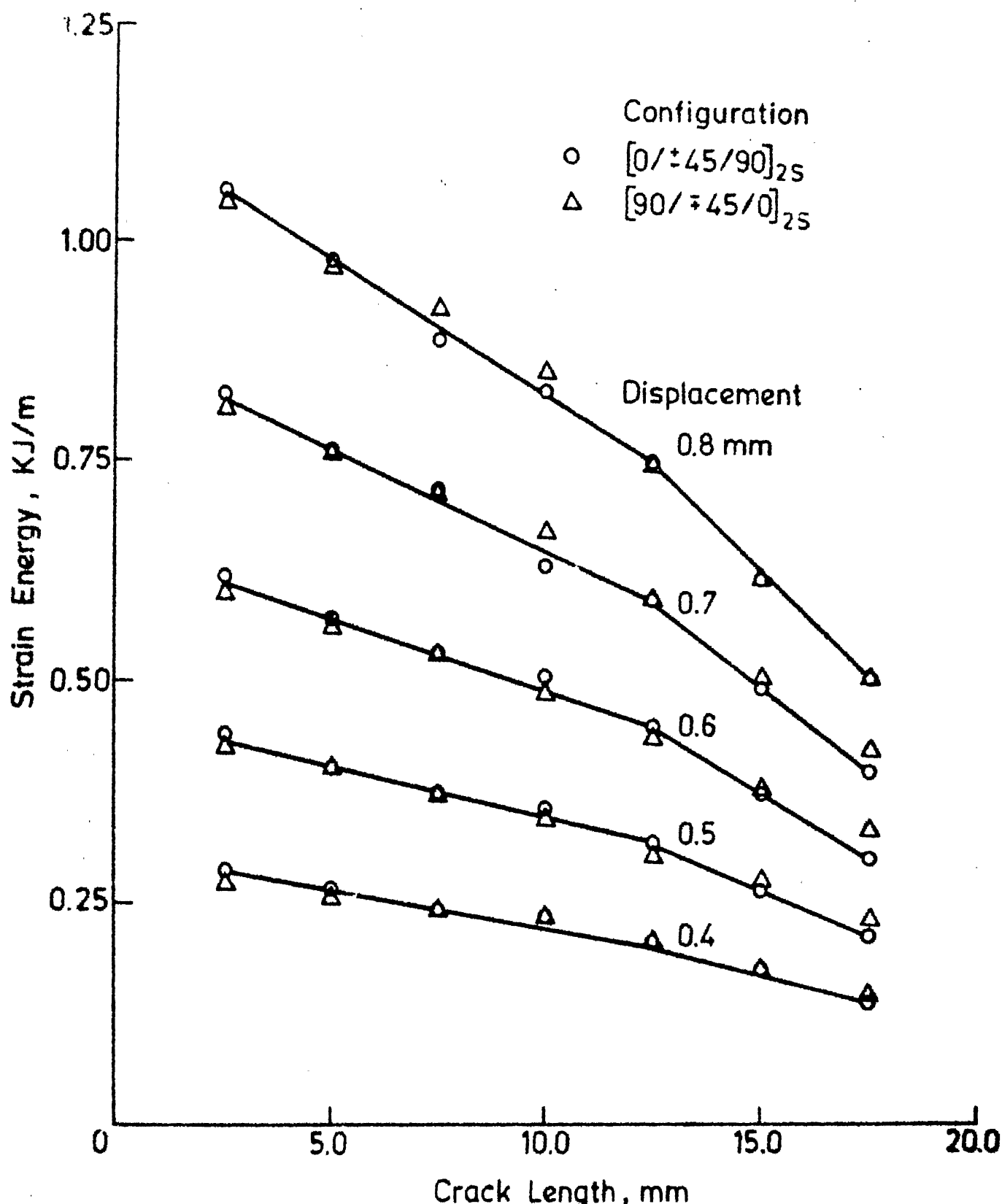


Fig. 3.5 Variation of strain energy per unit thickness with displacement for two different configurations.

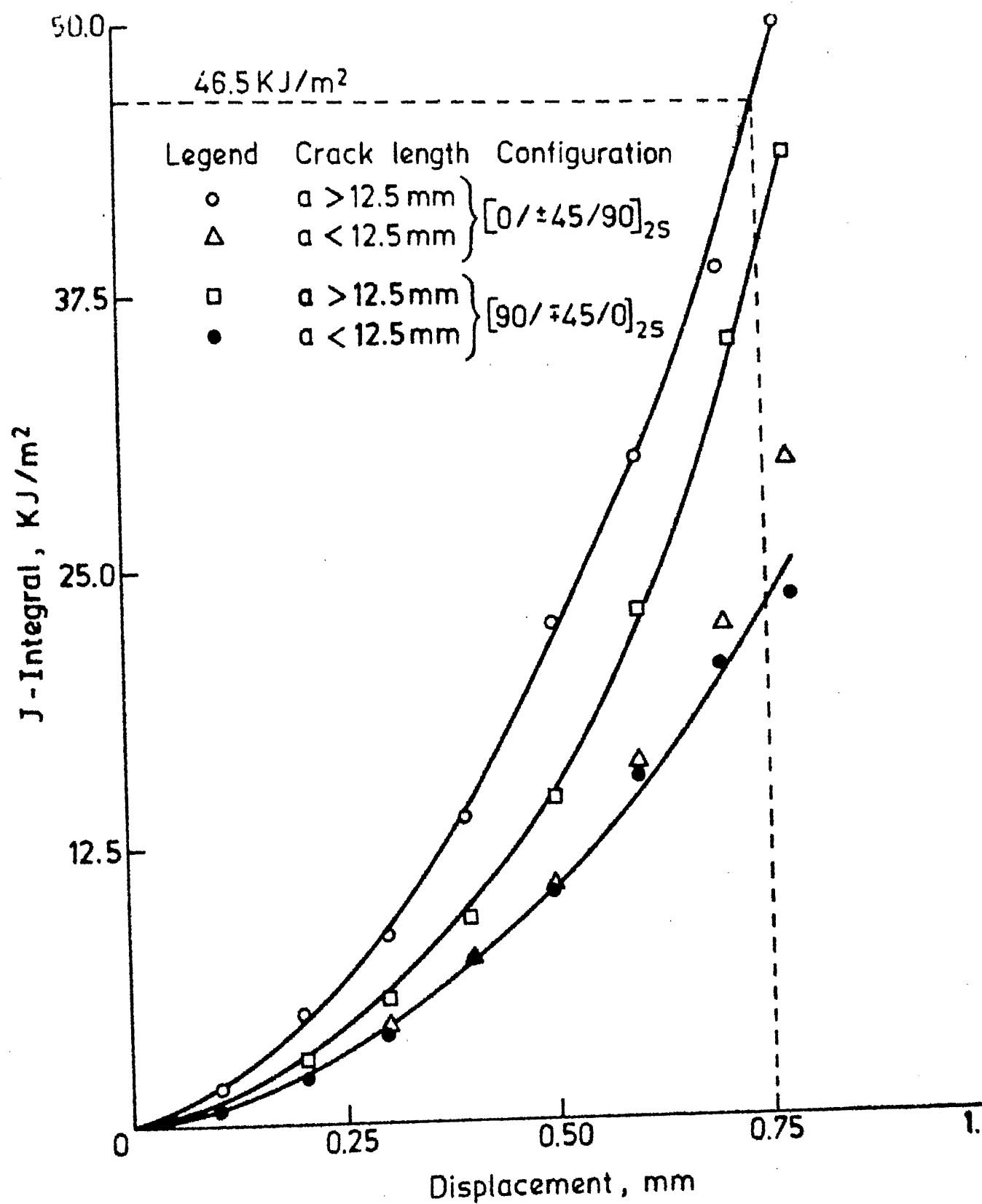


Fig. 3.6 J-Integral as a function of displacement for two laminate configurations.

errors. However in the lower ranges of crack length the critical displacement is more than 0.75 mm (for both the configurations Fig. 3.4) and that the J versus displacement plot (Fig. 3.6) does not extend to these values. Hence J_{1c} in the lower ranges of crack length cannot be determined. The applicability of J -integral in this range is discussed subsequently.

From the preceding discussion, it appears that when crack length is larger than 12.5 mm (or $a/W > 0.5$) the fracture behaviour is essentially governed by the crack tip environment resulting in a constant value of critical displacement and a critical value of J -integral can be determined. For these crack lengths, the fracture load is small which does not cause any material damage away from the crack tip region. On the other hand when the cracks are small ($a < 12.5$ mm or $a/W < 0.5$) the critical displacement depends upon the crack length indicating that in addition to the crack tip environment, the region away from it also influences such quantities as the energy absorbed and the displacement at fracture. This may be attributed to the fact that the fracture loads are high enough to cause general material damage.

In order to study the influence of general material damage in specimens with smaller cracks, additional specimens with varying specimen lengths were tested.

The length between the grips was varied from 3 to 6 times the width of the specimen. The load displacement behaviour for $[0/\pm 45/90]_{2s}$ configuration is shown in Fig. 3.7 for $l = 75$ mm and in Fig. 3.8 for $l = 150$ mm. These curves are similar to the ones discussed earlier (Figs. 3.1 and 3.2). The load at fracture increases slightly as the specimen length increases. Displacement at fracture (critical displacement) is plotted against specimen length in Fig. 3.9. As expected the critical displacement increases with specimen length for all crack lengths. The total displacement of the specimen is the sum of the displacement in the crack tip region, which may be independent of specimen length and displacement in the region away from the crack tip which should be a function of specimen length. The intercept on the ordinate obtained through extrapolation of a straightline in Fig. 3.9 may be regarded as the displacement in the crack tip region. When extrapolated to zero specimen length critical displacements fall in a narrow range of 0.575 mm to 0.675 mm. Essentially, this confirms the proposition [20] that the displacement could be taken as the sum of the displacement in the crack tip region which does not depend on specimen length and the displacement in the region away from the crack tip region which should be a function of specimen length.

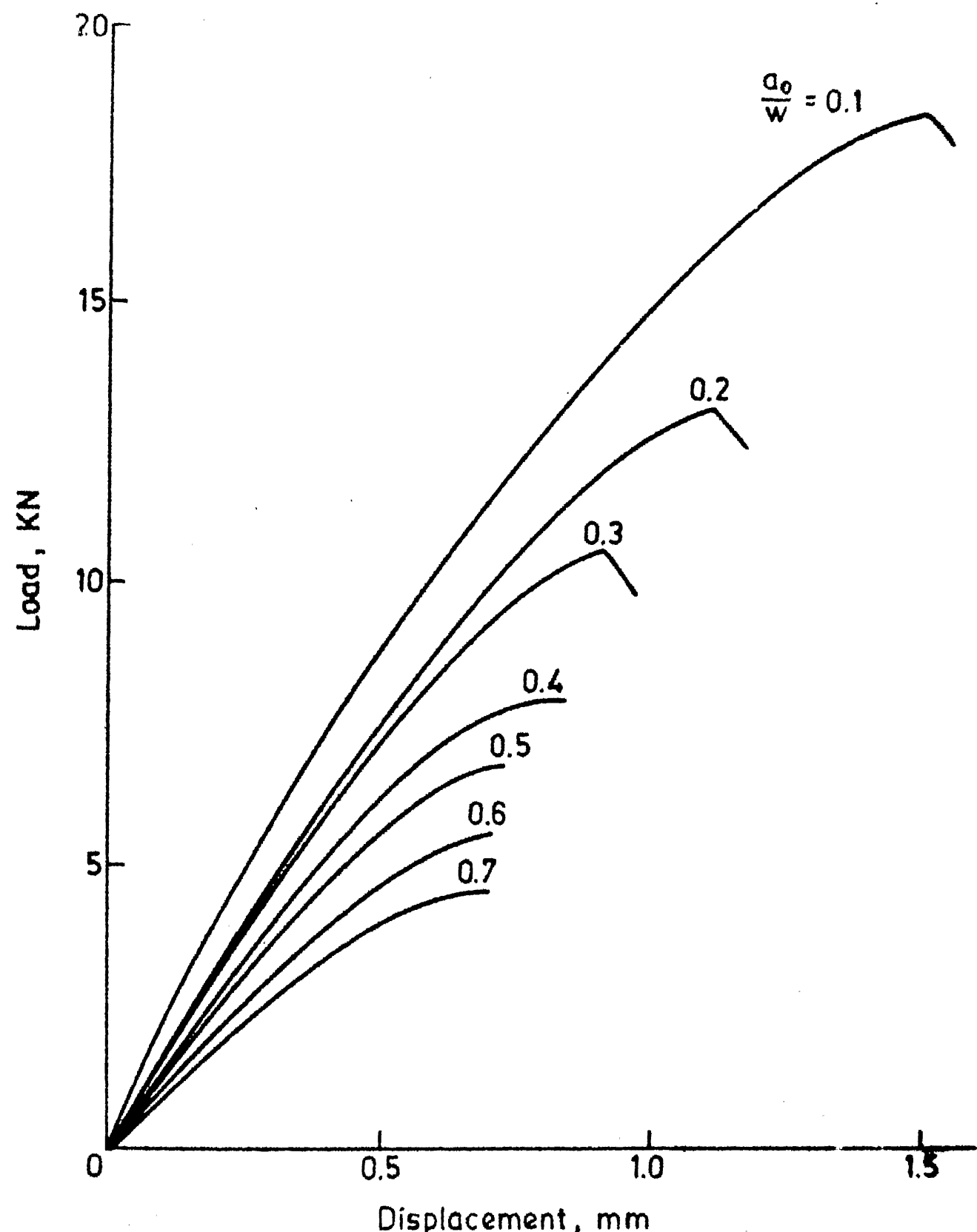


Fig. 3.7 Load displacement record for $[0/ \pm 45/90]_{2s}$ GFRP with $l=75$ mm.

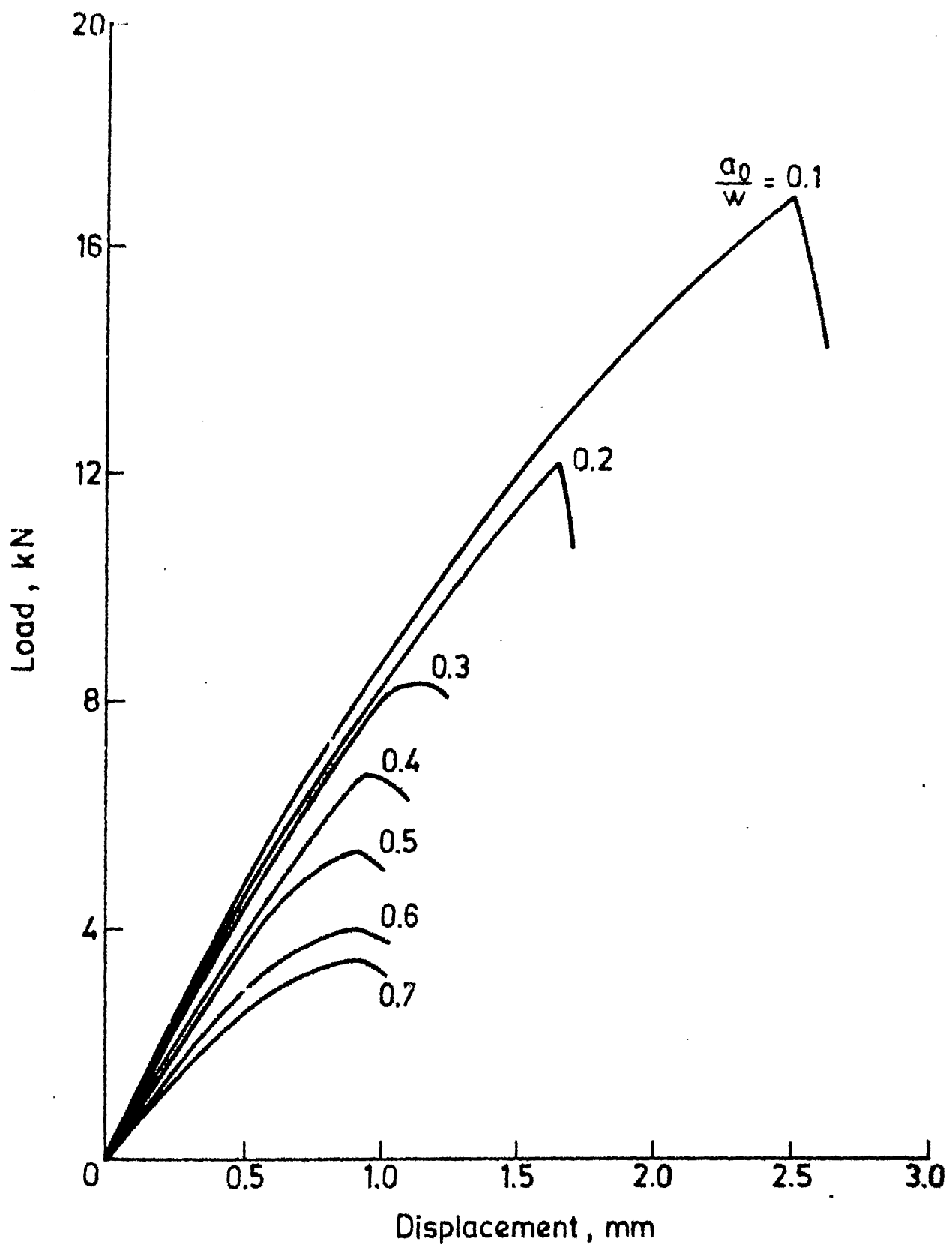


Fig. 3.8 Load Vs Displacement curve for $[0/\pm 45/90]_{2s}$ & $l=150\text{mm}$

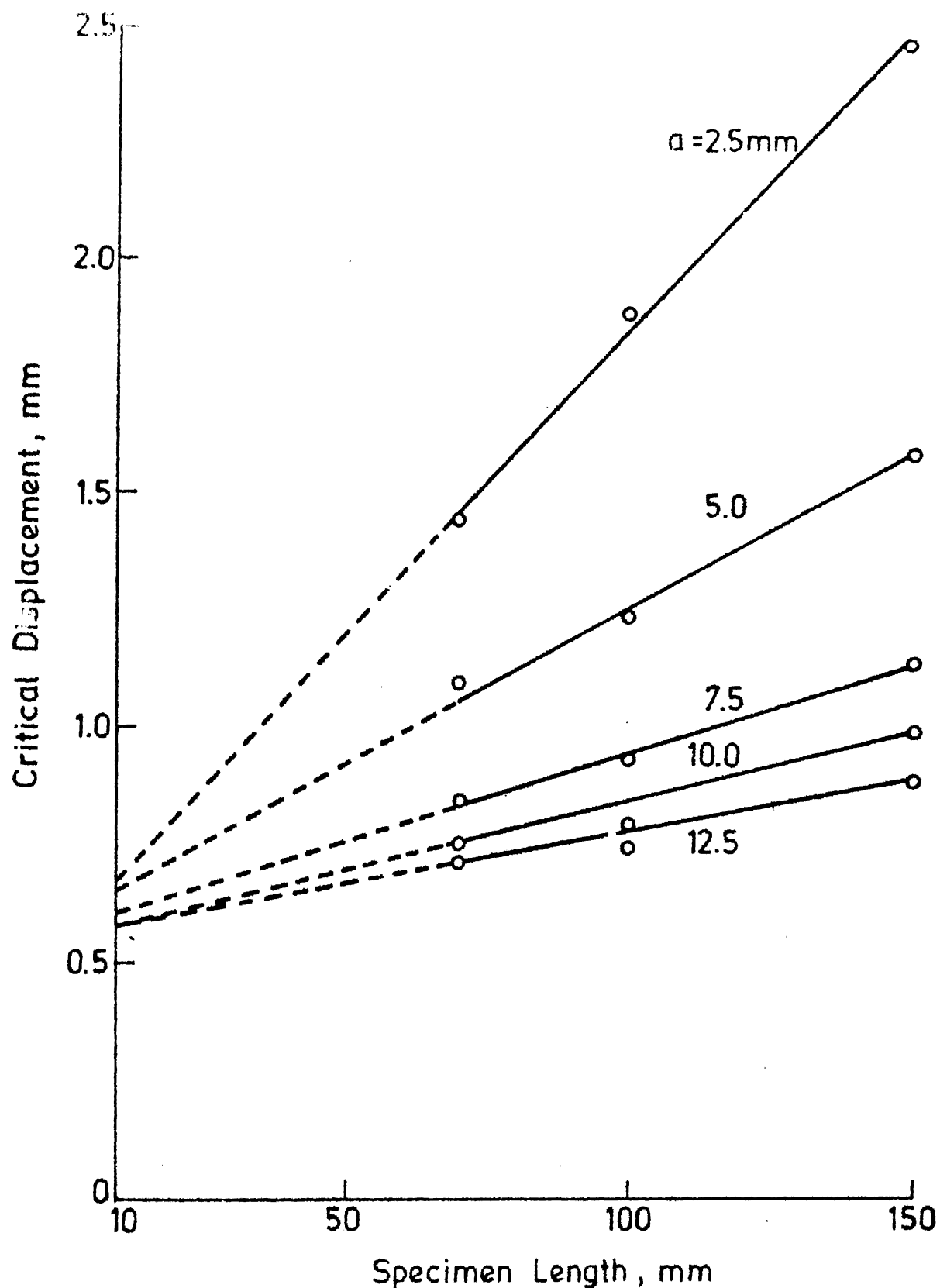


Fig. 3.9 Variation of critical displacement with specimen length for $[0/\pm 45/90]_{2s}$ GFRP.

Variations in the energy absorbed upto fracture are shown in Fig. 3.10 for different initial crack-lengths. The total energy may also be thought of as the sum of the energies absorbed in the crack tip region and the region away from it. The energy absorbed in the crack tip region should depend upon crack length but not on specimen length whereas the energy absorbed in the region away from the crack plane does depend upon specimen length. It is observed that when the crack length is 7.5 mm or more the energy absorbed is independent of specimen length signifying negligible energy absorption in the region away from the crack tip. For crack lengths of 2.5 and 5.0 mm, the total energy absorbed increases linearly with the specimen length indicating a significant energy absorption in the region away from the crack tip as well. These observations are further supported by visual observation of the specimens. The damage in the specimens with a crack length more than 7.5 mm is confined to the crack tip region whereas in specimens with smaller cracks the material damage is all over. This is illustrated in Fig. 3.3 through a photograph of two fractured specimens.

The intercept on the ordinate obtained by extrapolation of a straight line in Fig. 3.10 may be regarded as the energy absorbed in the crack tip region. Energy

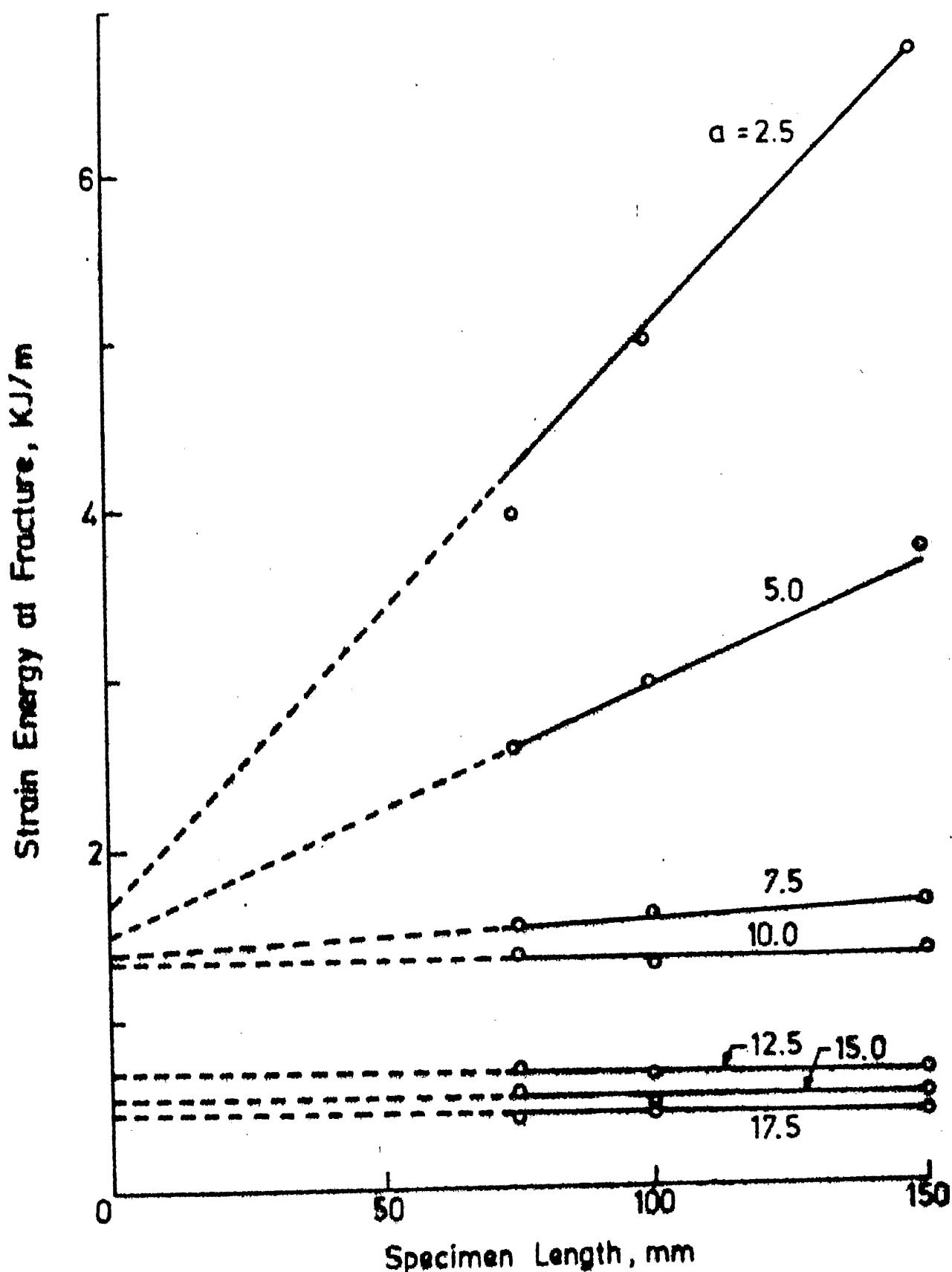


Fig. 3.10 Variation of strain energy with specimen length for different initial crack lengths for $[0/45/90]_{2s}$

absorbed thus obtained is plotted in Fig. 3.11. It was explained with respect to Fig. 3.9 that the critical displacement due to the presence of a crack alone is independent of crack length. Thus it may be argued that the energy absorbed for different crack lengths (Fig. 3.11) correspond to a critical displacement within a small range 0.575-0.675 mm and, therefore, the slope of the straight line may be used to obtain the critical value of J , independent of crack length. The J critical thus obtained is 43.04 kJ/m^2 which is close to the earlier obtained values of 46.5 kJ/m^2 and 41.0 kJ/m^2 (Fig. 3.6).

The load and load point displacement at fracture are nearly the same for $[0/\pm 45/90]_{2s}$ and $[90/\mp 45/0]_{2s}$ configurations. The J_{1c} values obtained are close to one another within the experimental error and the errors arising from manipulation of the curves during analysis.

3.2 CROSS-PLY LAMINATES

As a next sequence, cross-ply laminates of $[0/90]_{4s}$ configuration have been tested. Their load-displacement behaviour is shown in Fig. 3.12. As the specimen were loaded no damage could be observed till fracture load, whereupon catastrophic crack extension occurs and the specimen failed. Hence near the fracture load these do not show any load relaxation. Also the

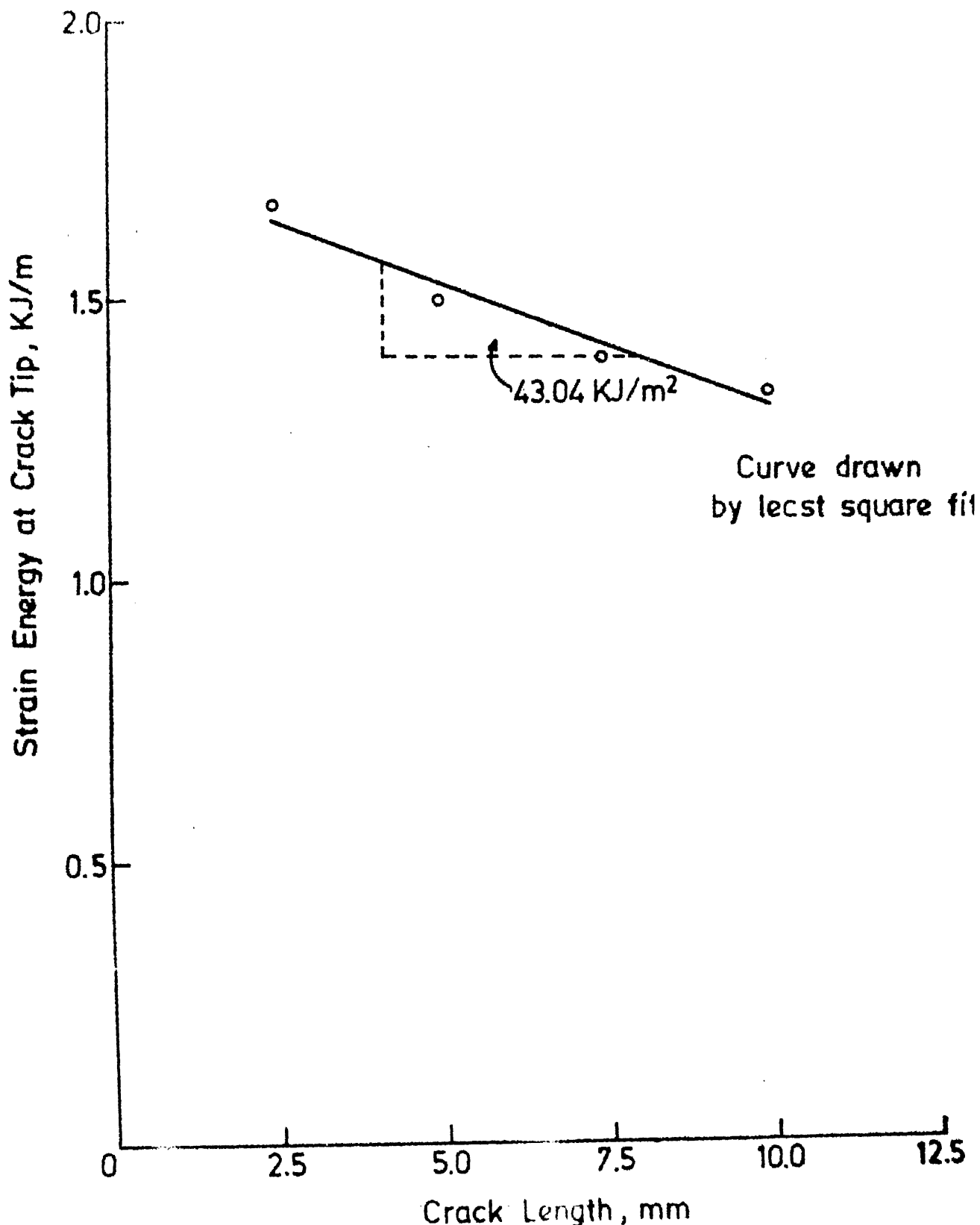


Fig. 3.11 Strain energy at the crack tip for different initial crack lengths for $[0/\pm 45/90]_{2s}$ GFRP.

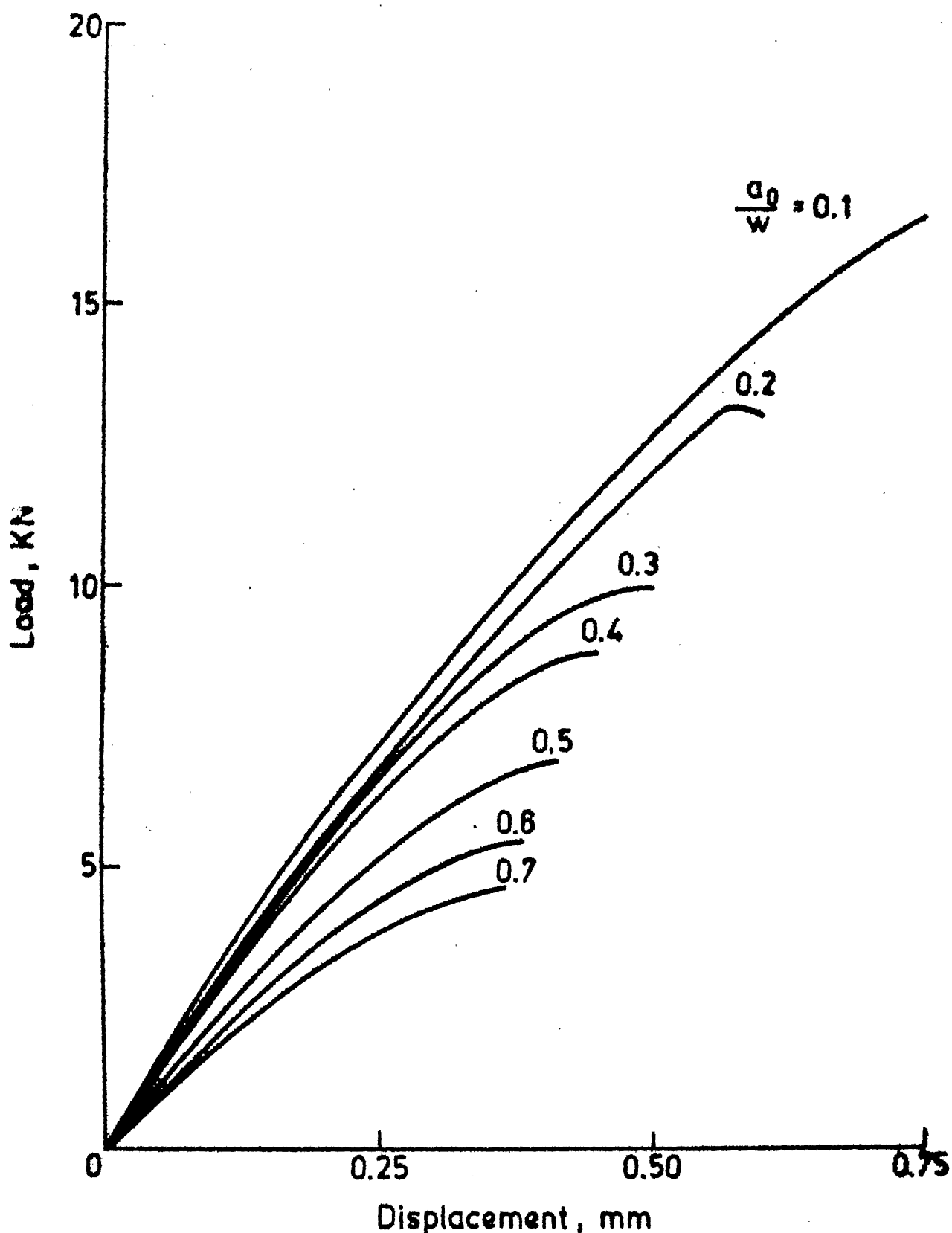


Fig. 3.12 Load displacement record for $[0/90]_{4s}$ glass fibre reinforced epoxy laminate.

displacements at fracture are lower than that for Quasi-isotropic laminates. The variation of critical displacement with crack length is shown in Fig. 3.13. The constant critical displacement is found to be 0.375 mm. This value is half of that for Quasi-isotropic laminates, implying that cross-ply laminates cannot withstand much displacement before the occurrence of fracture. Strain energy has been found out as the area under the load-displacement curves. This has been plotted against crack length for constant displacements at intervals of 0.05 mm (Fig. 3.14). This strain energy varies rapidly after $a = 10.0$ mm (or $a/W = 0.4$). The slopes of these curves have been found out and hence the J-integral has been plotted against displacement in Fig. 3.15. This curve is similar to that discussed earlier (Fig. 3.6). For the critical displacement of 0.375 mm the critical value of J-integral, J_{1c} is found out to be 22.65 kJ/m^2 , for $a/W \geq 0.4$.

In order to calculate J_{1c} , in the lower range of crack length, additional specimens of lengths 75 mm and 125 mm between the grips have been tested. The load displacement behaviour is shown in Figs. 3.16 and 3.17. The variation of critical displacement against crack length is shown in Figs. 3.18 and 3.19. The constant critical displacement increases with specimen length

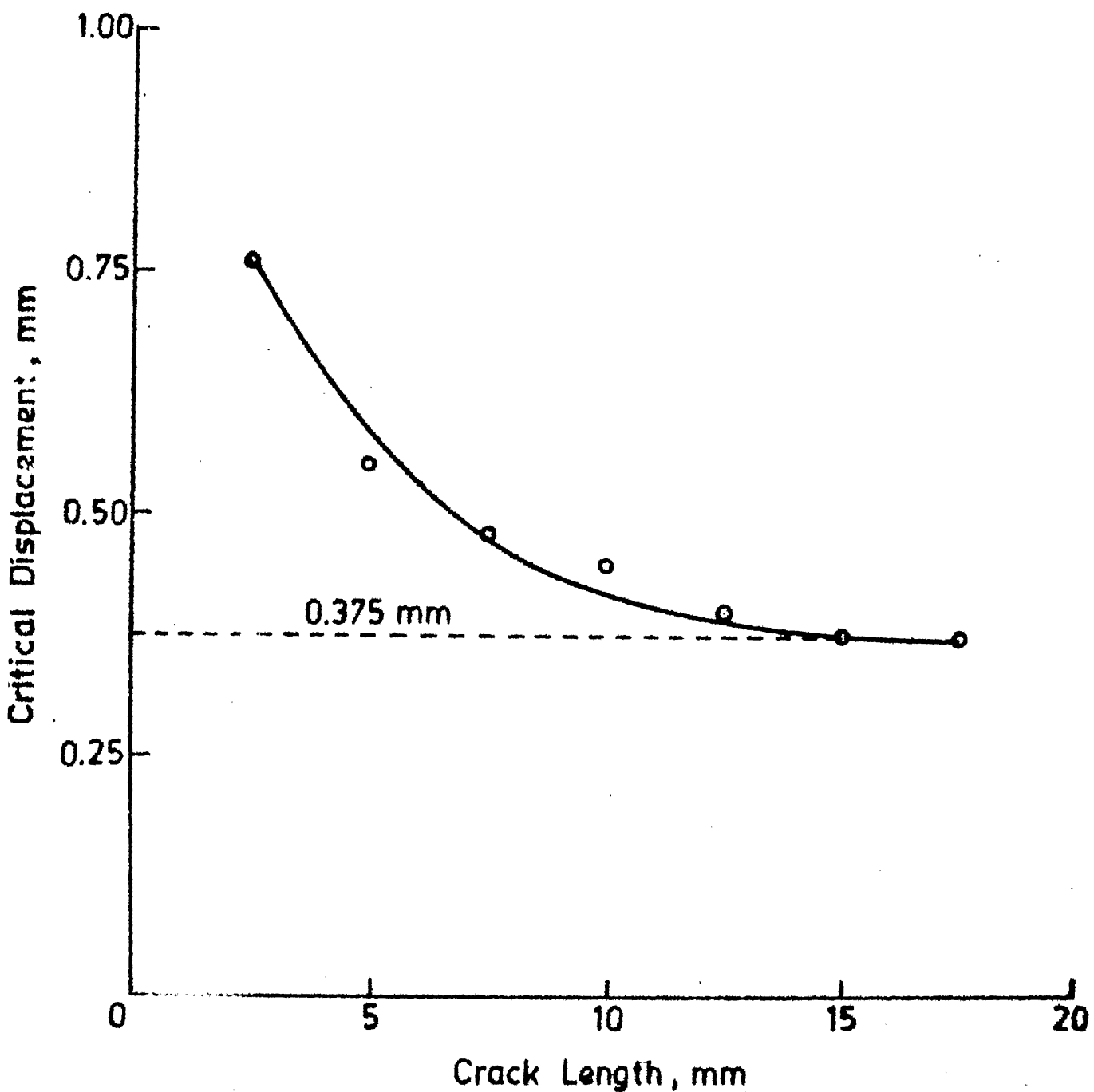


Fig. 3.13 Variation of critical displacement with crack length for $[0/90]_{4s}$ GFRP.

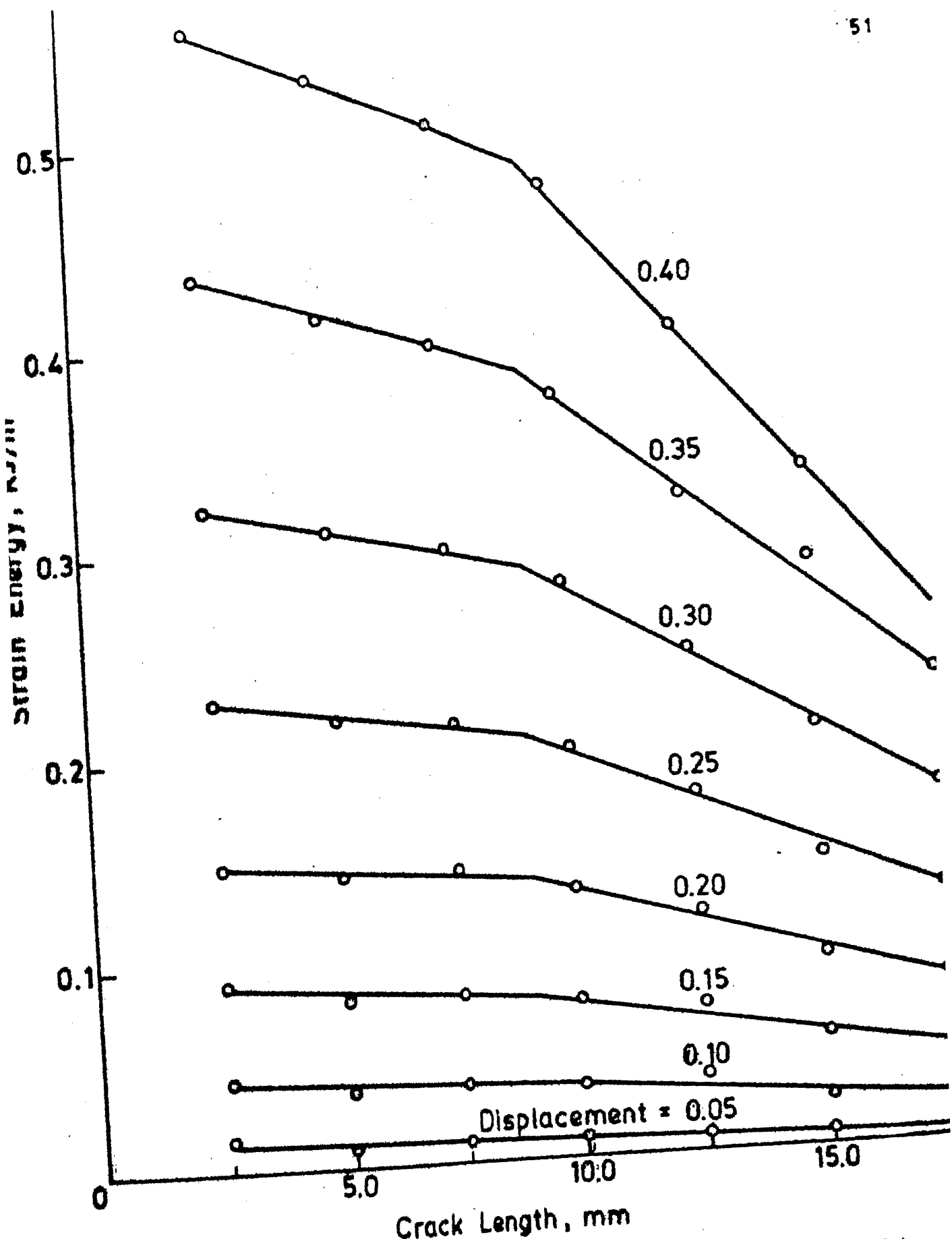


Fig. 2.14. Variation of strain energy per unit thickness with

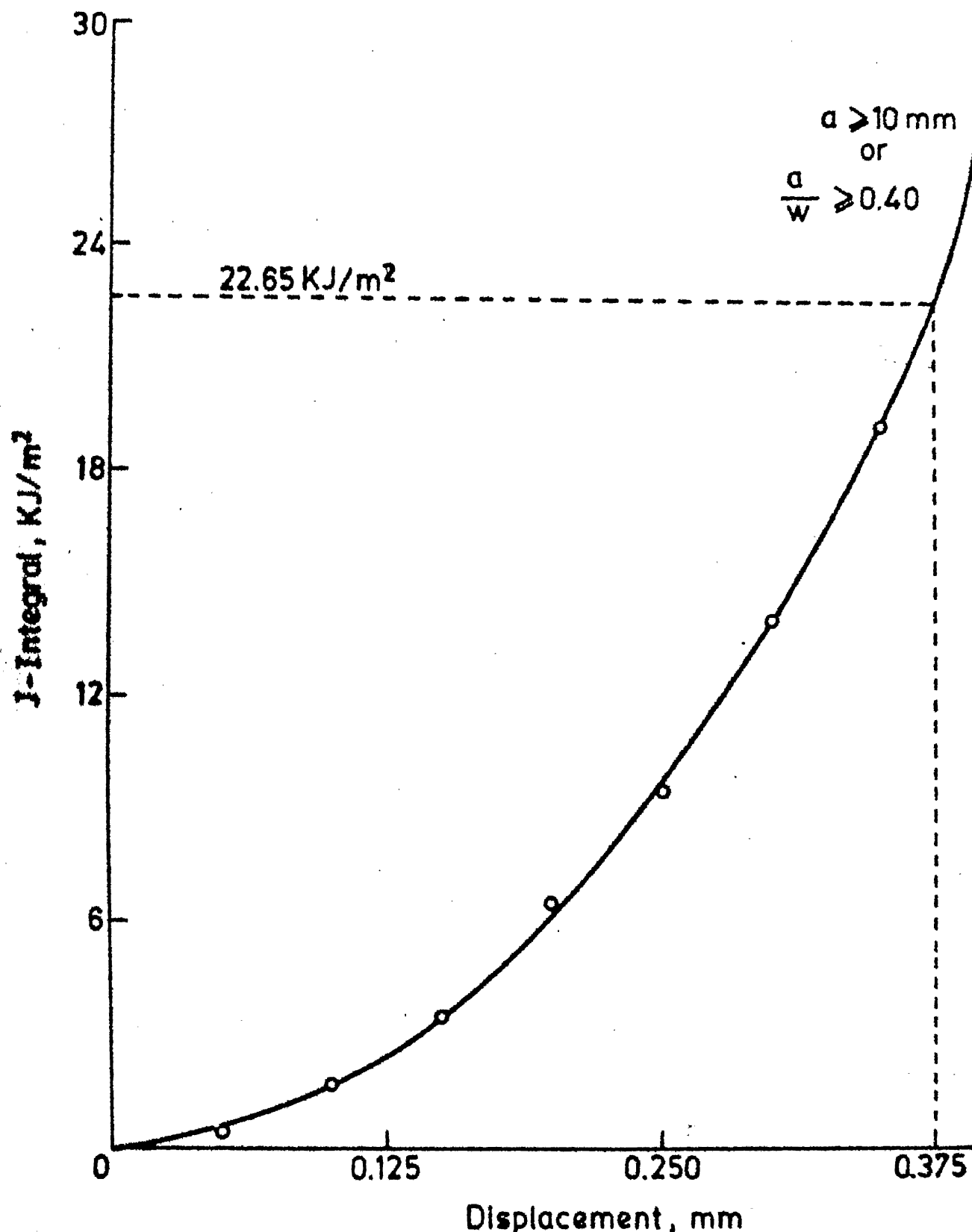


Fig. 3.15 J-Integral as a function of displacement for $[0/90]_{4s}$ GFRP.

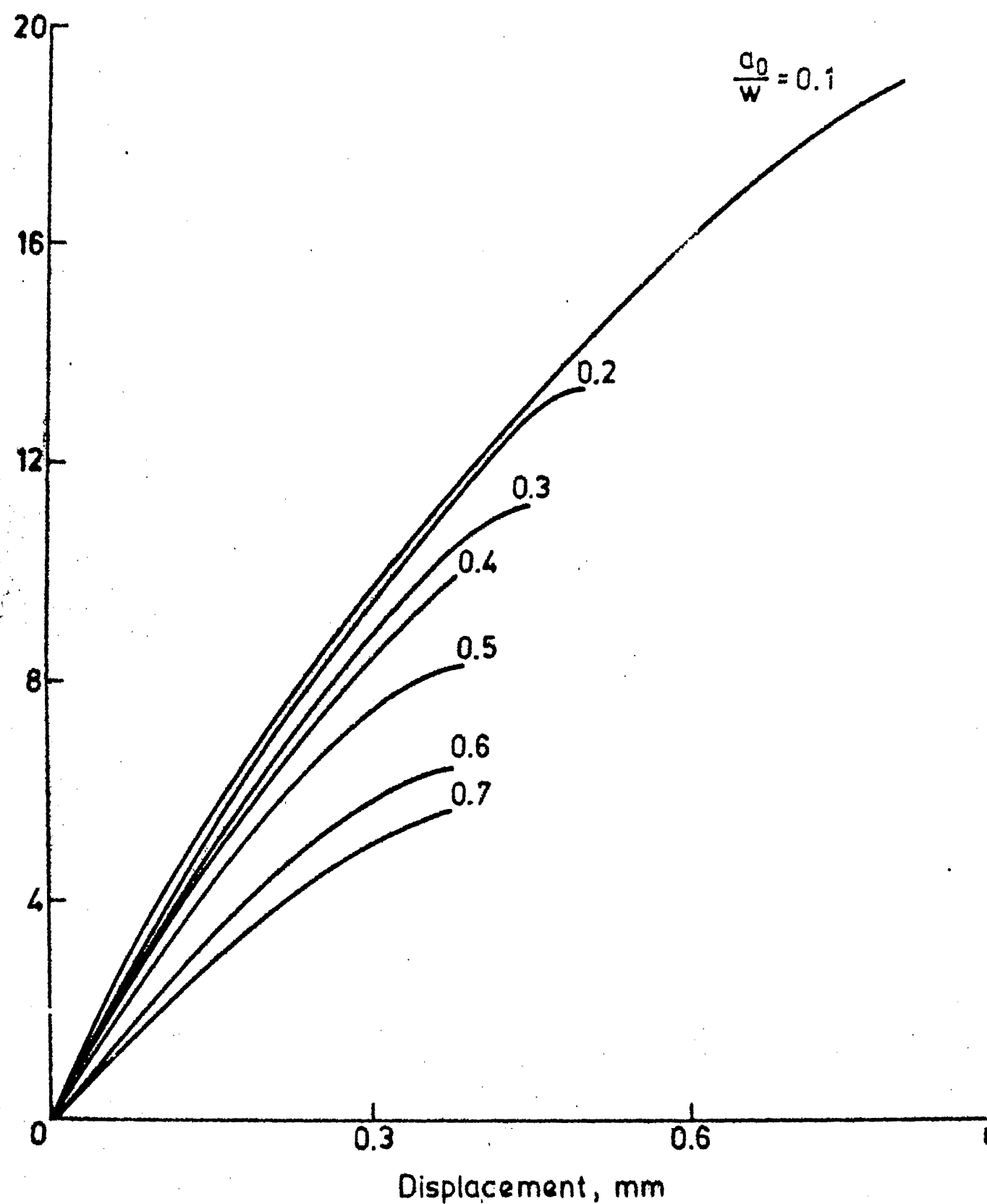


Fig. 3.16 Load-displacement behaviour for $[0/90]_s$ GFRP with

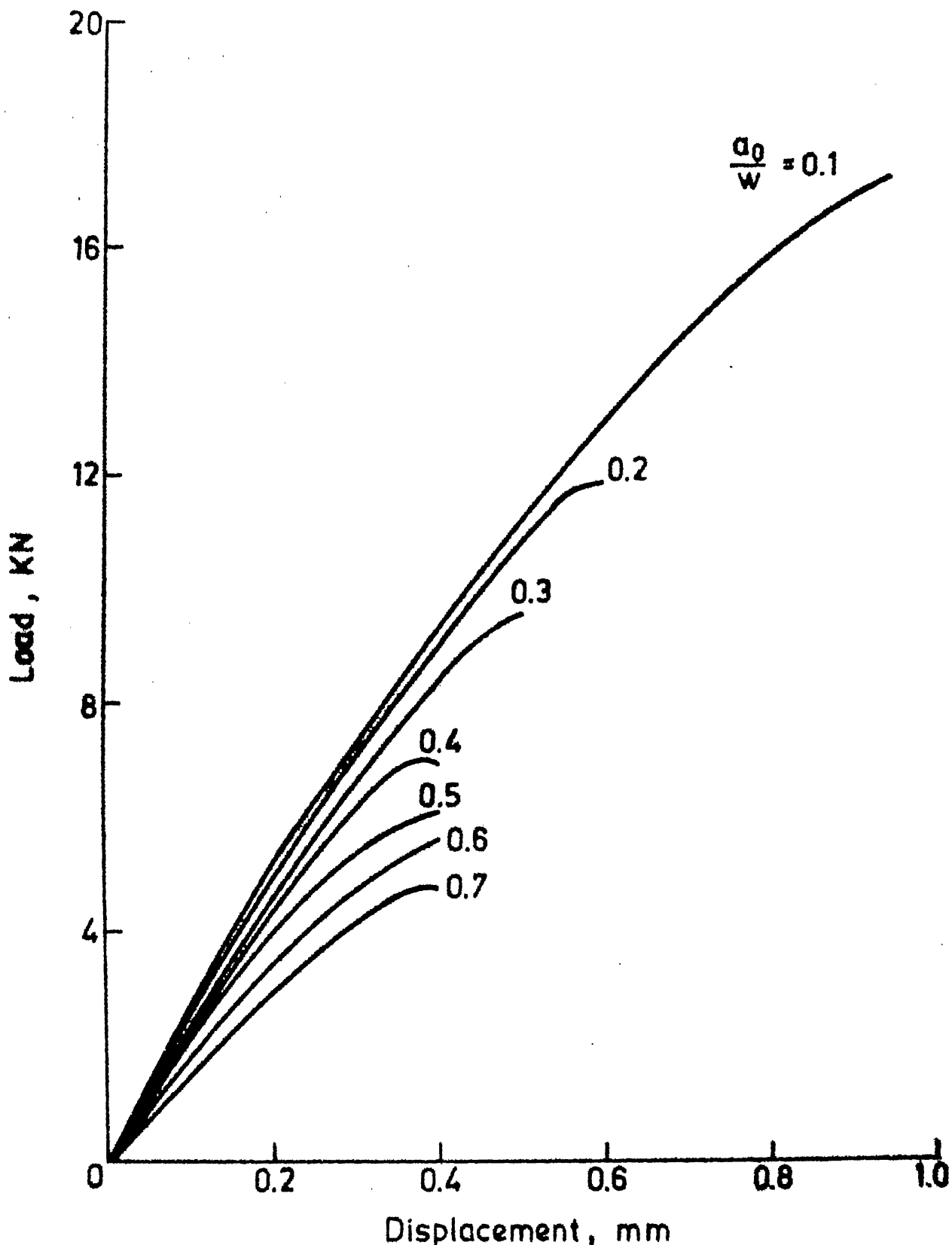


Fig. 3.17 Load displacement behaviour for $[0/90]_{4s}$ GFRP with $l=125$ mm.

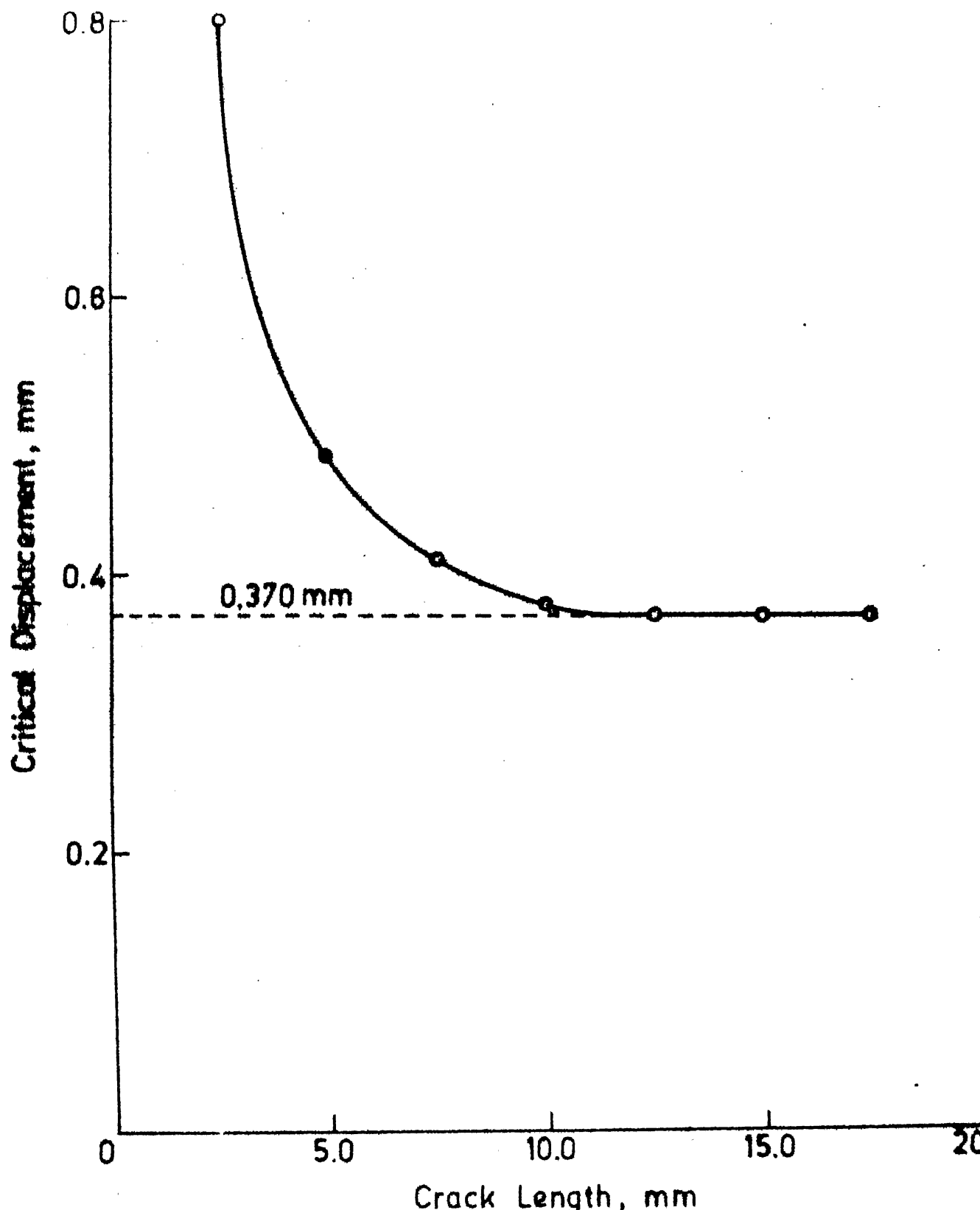


Fig. 3.18 Variation of critical displacement with crack length for $[0/90]_{4s}$ GFRP with $l=75$ mm.

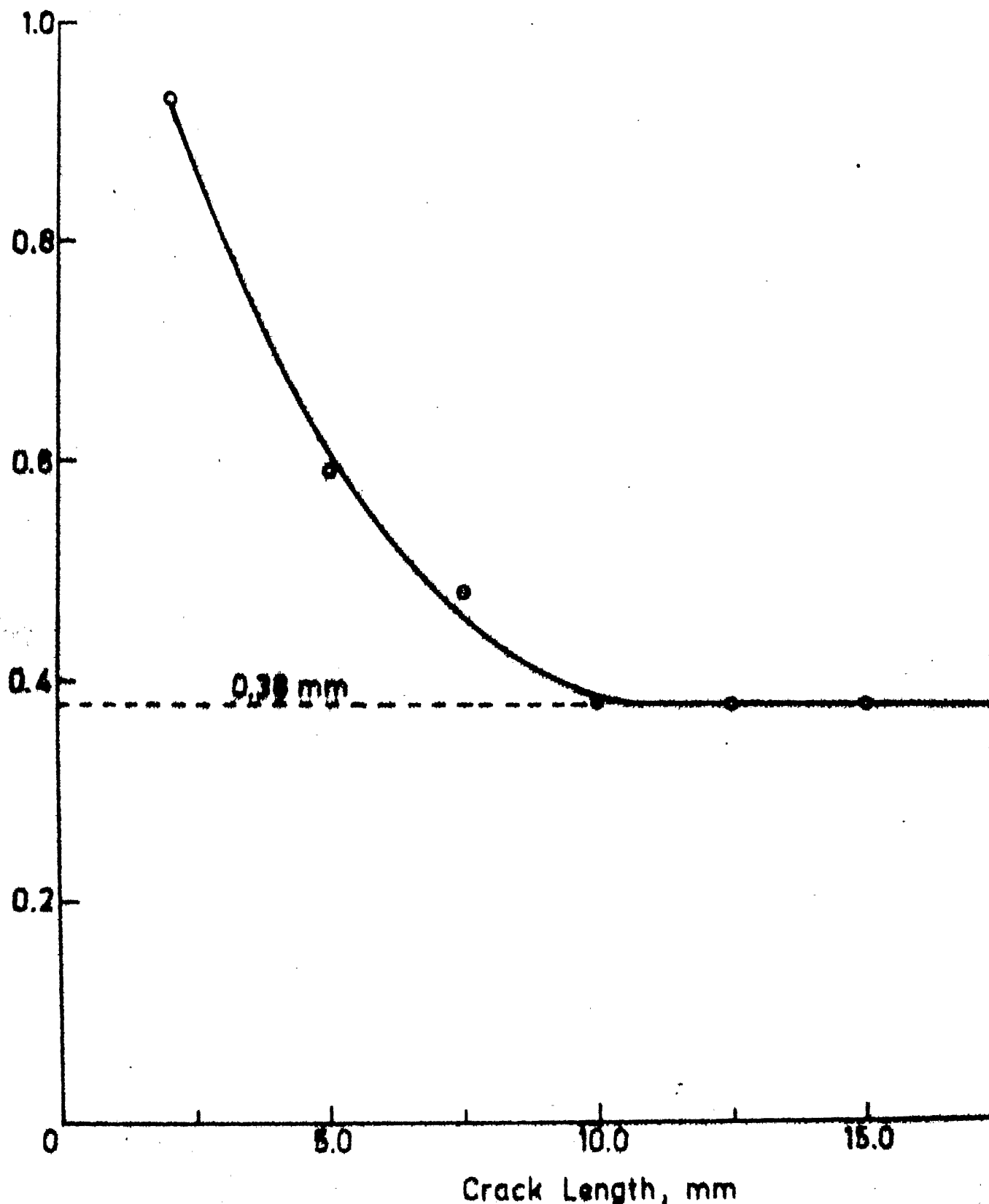


Fig. 3.19 Variation of critical displacement with crack length for [0/90]_{4s} GFRP with l = 125 mm

and is shown in Fig. 3.20. The plot of strain energy against specimen length for various crack lengths are shown in Fig. 3.21. These curves have been extrapolated for zero specimen length, which gives the strain energy at the crack tip. This strain energy at crack tip has been plotted against crack length in Fig. 3.22, the slope of which gives the value of J-integral at lower cracks. This is found out to be 22.2 kJ/m^2 , which is closer to $J_{1c} = 22.65 \text{ kJ/m}^2$ that obtained for higher crack lengths without extrapolation.

The properties of Quasi-isotropic and cross-ply laminates are summarised here for comparison.

	Quasi-isotropic	Cross-ply
Volume fraction, v_f	46.5%	43.5%
Ultimate tensile strength, σ_{LU}	240 MPa	405 MPa
Critical Value of J-integral, J_{1c}	46.5 kJ/m^2 (without extrapolation)	22.65 kJ/m^2 (without extrapolation)
	43.04 kJ/m^2 (By extrapolation)	22.20 kJ/m^2 (By extrapolation)

The J_{1c} value for cross-ply laminates is nearly half of that for Quasi-isotropic laminates although it has a higher value of ultimate tensile strength. At an outlook

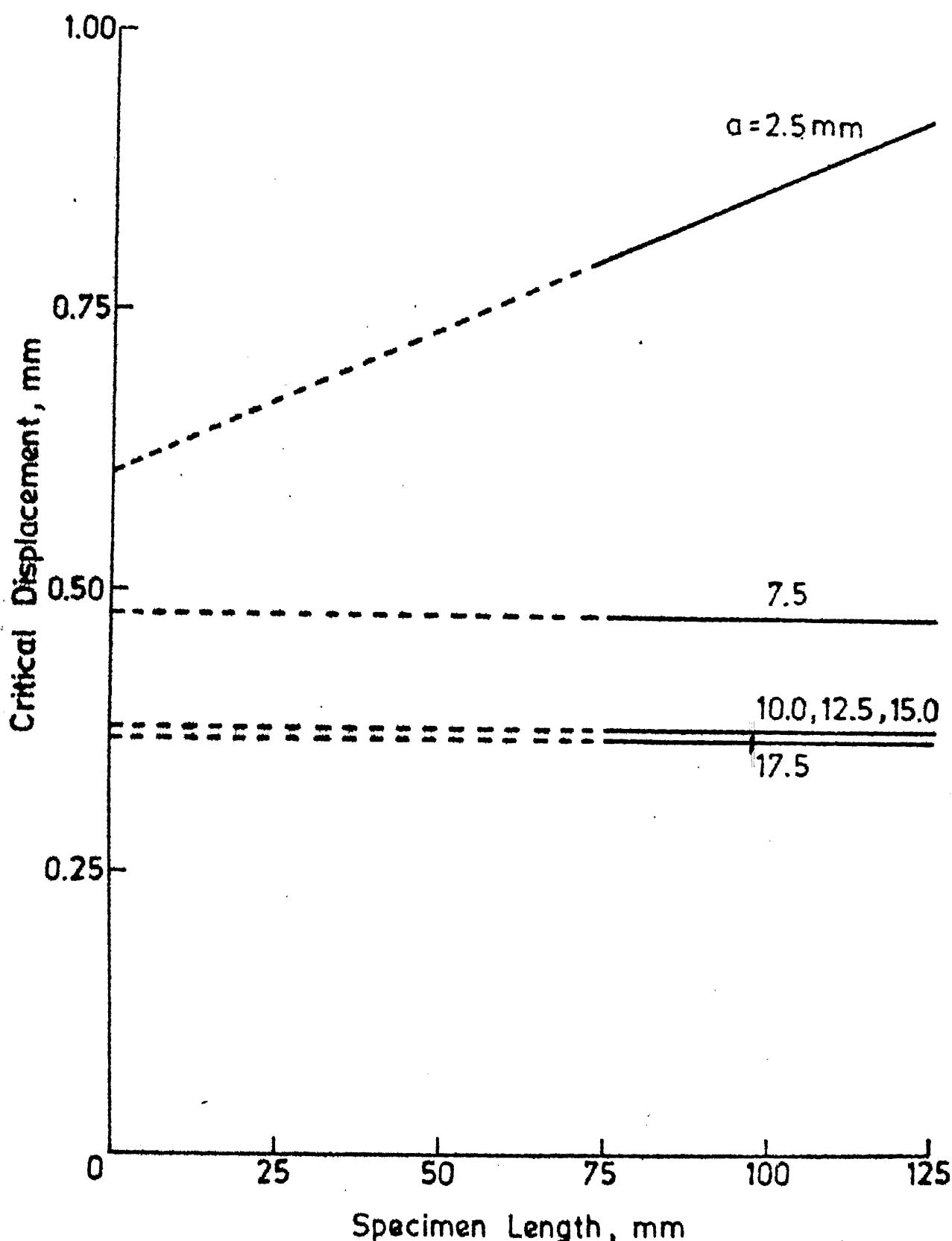


Fig. 3.20 Variation of critical displacement with specimen length for GFRP

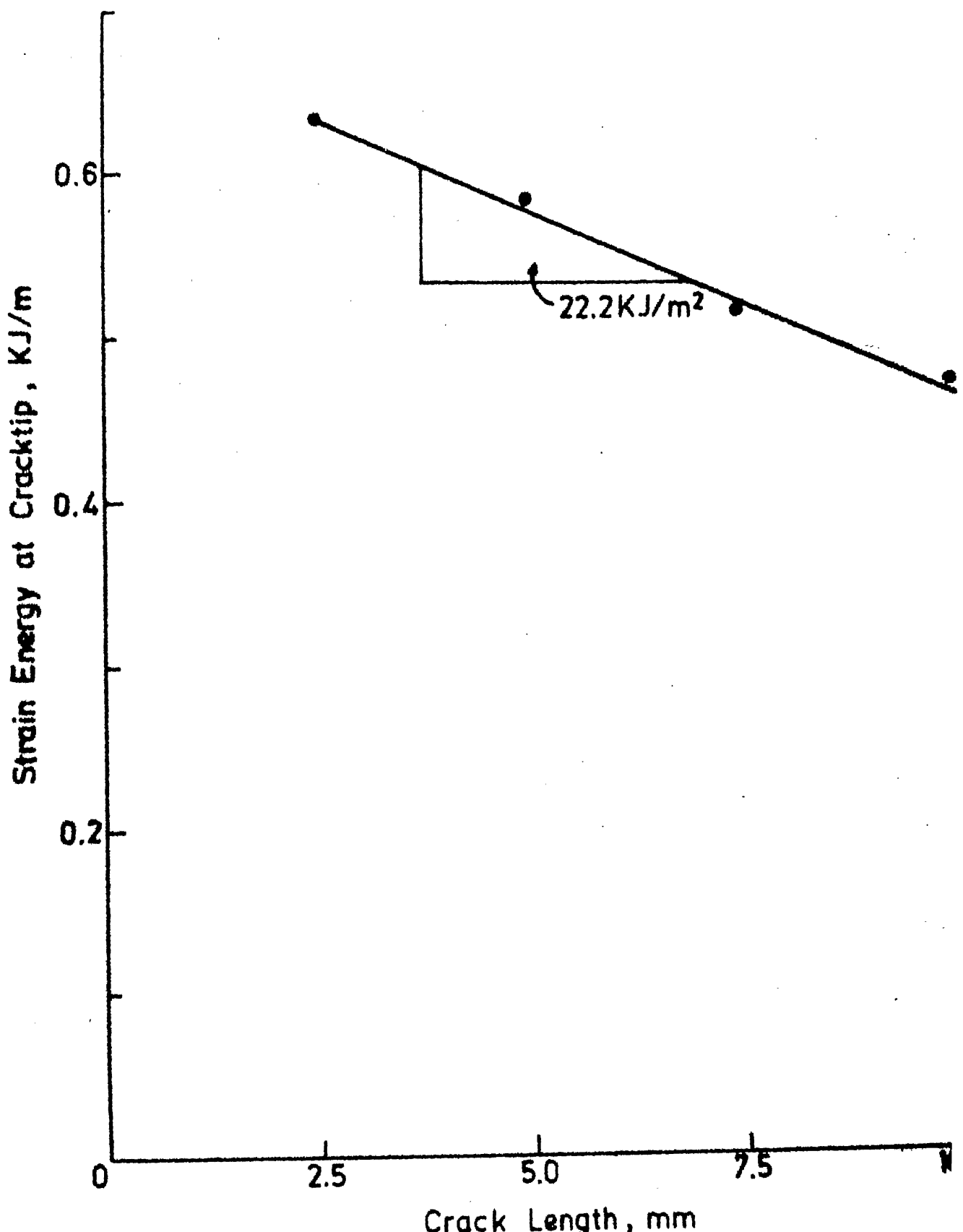


Fig. 3.22 Variation of strain energy at cracktip for different GFRP.

the results may seem bewildering. The reasons are explained subsequently.

3.3 FACTORS AFFECTING THE FRACTURE TOUGHNESS

As suggested by Mc Garry et all [21] the factors affecting fracture toughness are

- (i) Damage zone
- (ii) Stacking sequence.

3.4 DAMAGE ZONE

Anything that resists crack propagation shall enhance the fracture toughness. Damage zone is one such a parameter. The size of the damage zone is a measure of the fracture toughness. The more damage a FRP could sustain before failure the more its fracture toughness would be. In the present study it has been visualized that Quasi-isotropic laminates exhibit a bigger damage zone (Fig. 3.3) and hence a higher fracture toughness. On the other hand cross-plied laminates have a small damage zone (Fig. 3.23) and hence a lesser value of fracture toughness.

3.5 STACKING SEQUENCE

Stacking sequence plays a vital role in imparting the fracture toughness property of FRP. It has earlier been shown by Mc Garry et all [21] that the

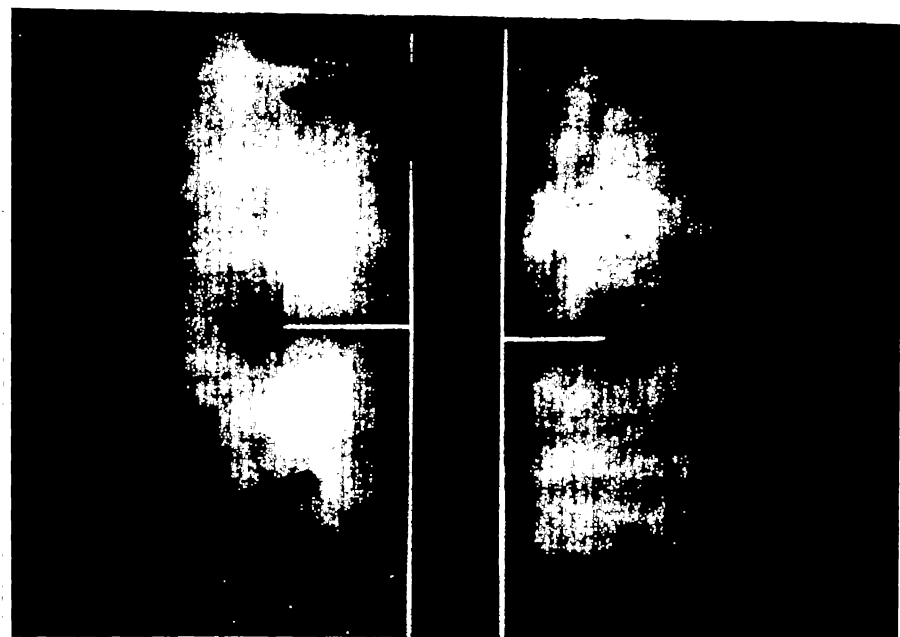


Fig. 3.23 : TRANSMITTED LIGHT PHOTOGRAPH OF
TWO SPECIMENS OF $[0/90]$ ₄₅
CONFIGURATION WITH DIFFERENT
CRACK LENGTHS.

$[+45]_{ns}$ laminates can withstand a stress higher than that predicted by ultimate tensile strength (for effective cross-section) whereas cross-plied laminates can withstand only less than half of that as predicted by ultimate strength. The case of Quasi-isotropic laminates has been shown to have a position in between these two.

When cross-ply laminates are stressed, the damage first occurs as subcracks in 0° plies formed by the inplane shear stresses and then in 90° plies because of the stresses σ_{xx} in 0° direction. As the load increases the cracks propagate along fibre directions in respective plies in a stable manner. A zone of delamination between 0° and 90° plies is formed at a higher load level. At a critical stress level, the fibres in 0° direction eventually fails and hence a catastrophic crack extension occurs. The inplane shear stress and inter-laminar shear stresses play a dominant role here and hence the earlier failure.

In the Quasi-isotropic laminates, upon loading subcracks form and spread along the individual plies. These subcracks (damage zone) spread along the entire thickness of the specimen and hence can take up a load comparable to that of the ultimate tensile strength and hence a higher value of fracture toughness.

3.6 CONCLUSIONS

Fracture behaviour of Quasi-isotropic and cross-plied laminates have been investigated. J-integral has been evaluated using the energy rate interpretation. Its value is found out to be independent of crack length when the ratio of crack length to specimen width (a_0/W) is larger than (i) 0.5 for Quasi-isotropic and (ii) 0.4 for cross-plied laminates. For smaller crack lengths general material damage away from the crack tip also influences the energy absorbed significantly. However, an extrapolation method as suggested by Patro [20] has been used through which the crack tip energy may be separated from the energy absorbed due to general material damage. The J-integral thus obtained is independent of crack length and specimen length and its critical value is the nearly same as obtained for (i) $a_0/W \geq 0.5$ for Quasi-isotropic and (ii) $a_0/W \geq 0.4$ for cross-plied laminates without extrapolation. It has been found out this method works excellently for the materials studied.

It is also seen that the size of the damage zone and the stacking sequence play a dominant role in characterizing the fracture toughness.

3.7 SCOPE FOR FURTHER WORK

The J-integral approach applied here to Quasi-isotropic laminates and cross-plied laminates shows a great promise. For greater confidence further investigations should be carried out using different materials and specimen variables. Some of the aspects which may be investigated are mentioned below:-

1. Influence of specimen width on J_{1c} can be tested for widths in the range 15 mm to 150 mm.
2. Influence of matrix material on J_{1c} may be investigated. Effect of thermosetting resins such as polyesters as well as thermoplastic matrices such as nylon, polypropylene etc. should be studied.
3. Influence of stacking sequence can be studied.
4. The J-integral can be applied to other reinforcement systems such as woven fabric. This is currently underway.
5. Influence of such environmental variables as moisture, saline water, acids and oils should be investigated. The effect of temperature on J_{1c} need be established.
6. Semi analytical methods should be devised so that an easier analysis can be made. One such a model is currently underway.

REFERENCES

- (1) S.K. Gagger and L.J. Broutman, "Crack Growth Resistance of Random Fibre Composites", *J. Composite materials*, Vol. 9, 1975, PP. 216-227.
- (2) S.K. Gagger and L.J. Broutman, "Effect of Crack-tip Damage on Fracture of Random Fibre Composites", *Materials Science and Engineering*, Vol. 21, 1975, PP. 177-183.
- (3) B.D. Agarwal and G.S. Giare, "Crack Growth Resistance of Short Fibre Composites:I - Influence of Fibre Concentration, Specimen Thickness and Width", *Fibre Science and Technology*, Vol. 15, 1981, PP. 283-298.
- (4) D.H. Morris and H.T. Hahn, "Fracture Resistance Characterization of Graphite/Epoxy Composites", Composite Materials Testing and Design (Fourth Conference) ASTM STP 617, American Society for Testing and Materials, Philadelphia, 1977, PP. 5-17.
- (5) J.R. Rice, "A Path Independent Integral and the Approximate Analysis of Strain Concentration by Notches and Cracks", *J. Applied Mechanics*, Vol. 35, 1968, PP. 379-386.

(6) J.W. Hutchinson, "Singular Behaviour at the End of a Tensile Crack in a Hardening Material", *J. Mechanics and Physics of Solids*, Vol. 16, 1968, PP. 13-31.

(7) J.R. Rice and G.F. Rosengren, "Plane-Strain Deformation Near a Crack Tip in a Power Law Hardening Material", I bid, PP. 1-12.

(8) F. McClintock, "Plasticity Aspects of Fracture", Chapter 2, Fracture, Vol. III, Ed. H. Liebowitz, Academic Press, New York, 1971, PP. 47-225.

(9) K.B. Broberg, "Crack Growth Criteria and Non-Linear Fracture Mechanics", *J. Mechanics and Physics of Solids*, Vol. 19, 1971, PP. 407-418.

(10) J.A. Begley and J.D. Landes, "The J-integral as a Fracture Criterion", *Fracture Toughness*, ASTM STP 514, American Society for Testing and Materials, Philadelphia, 1972, PP. 1-20.

(11) J.D. Landes and J.A. Begley, "The Effect of Specimen Geometry on J_{1c} ", Fracture Toughness ASTM STP 514, American Society for Testing and Materials, Philadelphia, 1972, PP. 24-39.

(12) J.D. Landes and J.A. Begley, "Recent Developments in J_{1c} Testing", Development in Fracture Mechanics Test Methods Standardization, ASTM STP 632, American Society for Testing and Materials, Philadelphia, 1977, PP. 57-81.

(13) B.D. Agarwal, B.S. Patro, Prashant Kumar, "J-Integral as a Fracture Criterion for Short Fibre Composites: An Experimental Approach", Paper accepted for publication in Engineering Fracture Mechanics.

(14) C.G. Chipperfield, "A Summary and Comparison of J Estimation Procedures", J. Testing and Evaluation, Vol. 6, No.4, July 1978, PP. 253-259.

(15) R.J. Bucci, P.C. Paris, J.D. Landes and J.R. Rice in Fracture Toughness, ASTM STP 514, American Society for Testing and Materials, Philadelphia, 1971, PP. 40-69.

(16) J.R. Rice, P.C. Paris, J.G. Merkle, in Progress in Flaw Growth and Fracture Toughness Testing ASTM STP 536, American Society for Testing and Materials, Philadelphia, 1973, PP. 231-245.

(17) J.D.G. Sumpster, C.E. Turner, in Cracks and Fracture, ASTM STP 601, American Society for Testing and Materials, Philadelphia, 1976, PP. 3-18.

(18) W.H. Bamford, A.J. Bush, "Fracture Behaviour of Stainless Steel", ASTM STP 668, American Society for Testing and Materials, Atlanta, 1979, PP.553-577.

(19) C.E. Harris and D.H. Morris, "The Effect of Laminate Thickness on the Fracture Toughness Behaviour of Composite Laminates", in Composite Structures (2), Edited by I.H. Marshall, Applied Science Publishers, 1983, PP. 511-523.

(20) B.S. Patro, "Experimental Studies on the Fracture Toughness of Short Fibre Composites", Ph. D. Thesis, Indian Institute of Technology, Kanpur, India, October 1983, PP. 124-133.

(21) F.J. Mc Garry, J.F. Mandell, S.S. Wang, "Fracture of Fibre-Reinforced Composites", Research Report R 76-8, M.I.T.